CERN/DRDC 92-44
LAA Status Report
3 September 1992

The Monte Carlo Simulation Laboratory (MSL) of LAA

F. Anselmo[§], F. Block[Δ], G. Brugnola[§], L. Cifarelli[*Δ§],
E. Eskut[◊], D. Hatzifotiadou[◊], G. La Commare[§], C. Maidantchik[◊°],
M. Marino[◊], S. Qian[◊], Yu. M. Shabelski[◊], G. Xexeo[◊°], Y. Ye[◊] and A. Zichichi[§]

Abstract

This report contains a summary of the main activities and achievements of the "Monte Carlo Simulations" component of the CERN LAA Project. These concern: i) phenomenological studies of possible Physics scenarios at future supercolliders such as LHC (16 TeV), SSC (40 TeV) and ELN (Eloisatron, 200 TeV) and ii) software tool developments for exhaustive Monte Carlo Simulations of complex events and detectors. The activities foreseen for 1993/94 are briefly reported.

(presented at the DRDC Open Session on 3 September 1992)

---

§ CERN/LAA Project, Geneva, Switzerland
Δ INFN-Bologna, Italy
* University of Pisa, Italy
◊ World Laboratory/HED Project, Lausanne, Switzerland
° COPPE/ Universidade Federal do Rio de Janeiro, Brazil

I. INTRODUCTION

Future experiments at hadron supercolliders, such as LHC (16 TeV), SSC (40 TeV) and ELN (Eloisatron, 200 TeV), will require intensive theoretical and phenomenological studies for extrapolations and predictions of the possible Physics scenarios, as well as detailed detector design studies to define the construction parameters needed. These studies have become one of the most important and challenging fields of today's High Energy Physics.

Besides the simulation of the so-called Standard Physics, also new and rare phenomena have to be considered such as, for instance, the production of the top quark, of the Higgs boson, of supersymmetric (SUSY) particles or the occurrence of B+L violation. Given the energy of future supercolliders, these phenomena would manifest in events with very high multiplicity (hundreds of particles per event) and would therefore be very complex to analyse.

Whatever is well established today (such as QCD and EW phenomenology) should be considered as the expected "background" for the next generation of supercolliders.

The task of the detectors which are going to operate at the energies of future supercolliders will be to select "interesting events" out of a huge amount of "background events" at a very high frequency (proportional to the luminosity). The detector design, its characteristics and performances will critically depend on the Monte Carlo simulations, as well as the future data analysis.

In this context, the activities of the MSL group of LAA have developed along the following two lines:

a) Phenomenological studies (section II);
b) Development of software tools (section III).

II. PHENOMENOLOGICAL STUDIES

1. Predictions for standard Physics at 16, 40 and 200 TeV

A study [1] aimed at giving reliable predictions for the bulk of soft inelastic interactions at future supercolliders has been carried out. The predictions of the Quark-Gluon String Model (QGSM) [2], a particular version of the non-perturbative Dual Topological Unitarization Model (DTU) [3], and of the QCD Lund Model [4], implemented via the program PYTHIA [5], for the inclusive spectra and multiplicity distributions of different secondary hadrons produced in pp or $p\bar{p}$ collisions in the energy interval $\sqrt{s}$ = 62 GeV–200 TeV have been studied: going from past and existing hadron colliders (ISR, Sp$\bar{p}$S, Tevatron) up to the "foreseen" ones (LHC, SSC, ELN). It has been found that both models describe reasonably well the existing experimental data. However, their predictions for the case of very high energies are somehow different. Figures 1-4 show some examples of predictions at $\sqrt{s}$ = 16, 40 and 200 TeV for the Feynman-x (x_F) distributions of charged hadrons (π, K, p) and for the total charged particle (N_{ch}) multiplicity in minimum bias (non elastic) events. The QGSM approach shows a faster decrease of the pion x_F-spectrum (figures 1a, 2a, 3a) due to the effect of multipomeron processes where softer secondaries are produced. Concerning the N_{ch} distribution (figure 4), QGSM predicts a relatively small contribution from diffraction dissociation and then a wide maximum with a long tail which corresponds to the overlap of contributions from different numbers of pomerons. PYTHIA predicts in turn a large contribution of diffraction dissociation and a relatively narrow peak from non-diffractive multiple interaction processes. All this reflects in different $\langle N_{ch} \rangle$ predictions from the two models, as shown in table 1.

Turning now to the "leading" hadron effect, in pp interactions the outgoing proton remains leading up to $\sqrt{s}$ = 200 TeV (see figures 1c, 2c, 3c and 5). The p$\bar{p}$ pair yield in the central region (being higher in QGSM than in PYTHIA) can increase with $\sqrt{s}$ (figure 5a) but the relative cross-section level for protons in the forward region remains practically the same both in QGSM and PYTHIA. In both cases, the x_F distributions in figure 5 almost scale with the energy. The same holds true for outgoing Λ_S baryons, when the light s quark is involved.

Also charm and beauty flavour production has been studied at various energies, comparing QGSM predictions with PYTHIA results obtained with different structure functions and K-factors[1]. A systematic study of 10 possible structure function parametrizations and three possible K-factors variants has been performed [6]. Figures 6-8 show the discrepancies existing between QGSM and PYTHIA already at low energies ($\sqrt{s}$ = 62 GeV and 630 GeV) when the x_F-distributions of charm and beauty mesons and baryons are compared, for a particular choice of K-factor and structure functions. QGSM seems to better reproduce the experimental data, as shown for instance in figure 6, and predicts the expected leading behaviour not only for strange but also for charm and beauty baryons (see figure 8) up to 200 TeV. In fact, besides the central production of heavy baryon pairs, the direct fragmentation of the initial baryon (p) into a heavy baryon, is treated in QGSM with string-junction conservation at the diquark level. Again the x_F distributions in figure 8 show very little scaling violations as $\sqrt{s}$ increases.

[1] The LO (leading order ~ α_s^2) contribution to the heavy flavour cross-section is multiplied by a K-factor to account for the NLO (non-leading-order ~ α_s^3) contribution, increasing the cross-section by 1.5÷3 times.

PYTHIA predictions obviously depend on structure functions. Although the results are similar at low energies, they become appreciably different at the energies of future supercolliders. In figure 9 the predictions in terms of N_{ch}, with three different (one "old" and two "new") sets of structure functions at $\sqrt{s}$ = 40 and 200 TeV, show the effect of structure function parametrization and the difficulty of long range extrapolations.

2. Heavy Higgs search at 16, 40 and 200 TeV

One of the main goals of future high energy colliders will be the search for the Higgs boson H^0. This is due to the crucial role this particle plays in the Standard Model (SM) which up to now describes experimental data very well.

There is no precise theoretical prediction for the Higgs mass. From experimental data (LEP) it is known that its lower bound must be around 59 GeV [7]. An upper bound can be theoretically derived by considering unitarity and gives about 1.2 TeV. Thus we are left with a wide mass range, open for speculations. We chose the *heavy Higgs case* ($m_H >> 2m_Z$) taking for the Higgs mass m_H = 500, 750 and 1000 GeV. In this case the preferred decay of the Higgs is into vector boson pairs (W or Z). A specially clean signal would presumably appear via decay chains containing the subsequent decay of the vector boson pairs Z^0Z^0 into muon pairs ($H^0 \to Z^0 Z^0 \to \mu^+\mu^-\mu^+\mu^-$).

The main processes for Higgs production at a given mass are gg fusion and W^+W^- fusion. The dominating irreducible background is due to all those processes generating Z^0 pairs subsequently decaying into four muons. The main contribution in the case of pp collisions comes from the continuum production of Z^0 pairs through gg fusion and $q\bar{q}$ annihilation.

Studies on Higgs particle detection at three energies (16, 40 and 200 TeV) have been performed. Here, again, the events were generated using PYTHIA. The corresponding cross-sections for signal and background are reported in table 2. Figures 10-12 show the results in terms of 4μ invariant mass spectra [8], when for instance cuts on the muon rapidity and transverse momentum, which could be feasible at the on-line level in an experiment, are applied. Notice that no cut on the Z^0 mass is performed. The effect of the experimental resolution has not been included: due to the broad width of the heavy Higgs[2], this is not critical and becomes negligible for $m_H > 750$ GeV. The spectra refer to four years of running at 10^{34} $cm^{-2}s^{-1}$ luminosity. The following inputs were used: m_t = 130 GeV, $BR(H^0 \to Z^0Z^0) = 0.3$ and $BR(Z^0 \to \mu\mu) = 0.03$. The message is clear: the higher is $\sqrt{s}$, the better a heavy Higgs is observable. In particular, for $m_H >$ 500 GeV, Higgs detection at LHC appears really critical. Of course, other cuts to

[2] $\Gamma_H = 0.5 \text{ TeV} \left(\frac{m_H}{1 \text{ TeV}}\right)^2$

enhance the Signal/Background (S/B) ratio, in particular concerning the p_t of the Z^0s, have been investigated [8].

In addition we have studied a new approach to the problem with the help of a neural network (NN) [9]. The idea is to use the NN as a "feature extractor" to derive event signatures that could be implemented in an experiment at a high-level of trigger. We use PYTHIA to generate Higgs and background events, containing four muons as above, and the package JETNET [10] for NN simulation. Each event is analysed as a whole (using the p and p_t information of all tracks) and a set of significant variables to be fed to the NN is chosen. This essentially consists in the p and p_t (with respect to the jet axis) values of the fastest four particles of the fastest jet in the event. Then the NN is trained on two sets of Higgs and background events (training sets) to *learn* the difference between both event types. Once training is completed, new events (not contained in the training sets) are presented to the network and its quality of performance is estimated. The results obtained with the NN for the case of $m_H = 750$ GeV are shown in figure 13. The trend seems to be the following: a good Higgs selection corresponding to a good level of purity[3] or, say, to a good S/B ratio, can be achieved with the NN approach at high efficiency[4] levels. This is of course of great relevance in those conditions (of m_H or $\sqrt{s}$) where the Higgs cross-section is really small. Work is in progress to understand how the NN performs with respect to the "traditional" analysis method when the same input variables are used and the best compromise between purity and efficiency is achieved in both cases.

3. The effective threshold for SUSY breaking

Where the effective threshold for Supersymmetry breaking is, i.e. at which level of energy the lightest sparticle could show up, is a fascinating question. We have devoted a lot of effort understanding this problem [11-17]. Figure 14 summarizes our results. Our conclusion is that, given the theoretical uncertainties and experimental errors of all the Physics ingredients needed in this analysis (in particular, the new LEP measurements of $1/\alpha_{em}$, α_s and $\sin^2\theta_W$), it could very well be that SUSY breaking is "around the corner": already at the energy level where LEP I, Tevatron, HERA or LEP II are operating or will start to operate. Of course, given the spread of the SUSY particle mass spectrum (see the examples in figure 15), supercolliders will be essential to explore the Superworld.

4. Detector Simulations

Monte Carlo Simulations in a full coverage, complex detector consisting of different elements are not an easy task. Figure 16 shows an example of Higgs event at $\sqrt{s}$

---

[3] $\text{Purity} = \dfrac{\text{Higgs events}}{\text{Higgs events + background events}}$ after cuts.

[4] $\text{Efficiency} = \dfrac{\text{Higgs events after cuts}}{\text{Initial Higgs events}}$.

= 40 TeV displayed in the so-called "LAA test detector". This is essentially made of a central tracker followed by an e.m. + hadron calorimeter and by a muon absorber + tracker (the latter also in the forward region), with inner (for central tracker) and outer (for μ tracker) magnetic field options. The event was generated with PYTHIA and tracked with the well-known GEANT package [18]. The task of the MSL Group has been so far to act as a consultant for the various components of the LAA Project (scintillating fibre tracker, noble-liquid calorimeter, "spaghetti" calorimeter, muon detector), thus providing the appropriate generated events samples and software tools (see section III) for simulation. In addition, these various components are being assembled in a unique set-up configuration where the following problems are being addressed, in particular concerning the Higgs search via μ detection:

- magnetic field options;
- particle ranges;
- punch-through effects;
- track (and vertex) finding algorithms.

However the problem of minimizing the GEANT running time when multitask performances are required (tracking with multiple scattering, energy loss, shower production, digitization of hit points) is still a major problem despite the efforts of the computing community so far.

III. DEVELOPMENT OF SOFTWARE TOOLS

As already mentioned, the MSL group has also treated technical problems, related to the software needed for Monte Carlo simulations. As the energy and multiplicity of events increase with energy also the detector size and complexity increase. All this translates into huge software packages, whose organisation, handling and mutual linking becomes very difficult. The problem critically shows up when different event generators have to be interfaced to different detector simulation and/or analysis programs. Only recently Monte Carlo authors agreed on the introduction of some standards. Below we give a list of items on which the group has so far focused its activities.

1. Monte Carlo Event Generator Adaptor (MEGA)

A solution to the problem of standardising the data structure for the output of Monte Carlo event generators has been worked out, which is by far more complete than a simple output commonblock. It consists of a package of routines, collectively called MEGA (Monte Carlo Event Generator Adaptor) [19], which provides a unique standard database for all the different existing event generators. MEGA is internally organised via ADAMO [20], a modern data structure system based on the Entity-Relationship model. Data are treated as "entities", with their "attributes", and mapped onto tables which can be comfortably handled for any further application (see figure 17).

2. Full Monte Carlo Chain (FMC)

An immediate application of MEGA is in fact the FMC (Full Monte Carlo Chain) [21] package, where MEGA is interfaced with GEANT to allow particle tracking inside a detector. The MEGA tables are used as input, then updated in output with the results from the tracking for further analysis. Figure 18 illustrates the FMC structure. A more detailed description can be found in the most recent LAA Report [22]. The current FMC version 1.3 uses ADAMO version 3.0 and is implemented on both IBM/VM and VAX/VMS.

3. Set-Up Descriptor (SUD)

A few years ago, due to the lack of suitable interactive tools to access the GEANT program, a new package was written, the so-called SUD (Set-Up Descriptor) [23], in order to set up the geometry of the detector for FMC. SUD generates a Generalized ADAMO File (GAF) where the detector data are mapped according to the GEANT geometry. SUD exists in both batch and interactive versions. In particular, the interactive version constitutes a very user-friendly tool. It is operated via menus based on the KUIP [24] command interpreter and gives various possibilities: to describe detector volumes, to define materials and tracking media, to position the volumes, to divide them into sections, etc.. SUD runs on VAX/VMS, but ADAMO tools exist for "exporting" the generated GAF to a machine-independent file and "importing" it into another computer (i.e. IBM/VM, UNIX platforms).

4. Particle Decay Data Base (PDKDB)

A Particle and Decay Channels Data Base (PDKDB) [25] has been developed, to manage the information on particle properties and their decays, which again uses the ADAMO Entity-Relationship model. The data are obtained from the Particle Data Group (PDG), with whom a collaboration has been established. The aim is to produce a scheme for an automatic update of some universally accessible file, with the latest (yearly updated) information on particle properties, to be extensively used in any Monte Carlo or analysis program.

5. General purpose facilities

The Comprehensive Application Builder (CAB) [35] system is being developed to help the physicists to build FORTRAN programs using different subroutine libraries. Its task is to reduce the effort when selecting and connecting subroutines and functions in a working program. The system has a graphic window to define data flow diagrams, one of the most successful Software Engineering methods, which can be used to derive the programs almost automatically.

The Software Information Manager (SIM) [36] is a tool to handle source code and its documentation in a unique framework. Integrated in the CMZ environment, SIM provides guidelines to generate the "program maintenance manual" and the "user manual".

6. Graphics Development

The increasing power of graphics systems has made it possible to start a new project concerning the detector design. The commercial product Application Visualisation System (AVS) has been chosen due to its user-friendliness. Few weeks after the installation of AVS on our platforms (HP 7xxs), a set of modules has been defined mapping the various GEANT shapes and using the same parameters as in GEANT. Work is in progress to describe the whole geometry package (positioning, divisions, rotations, etc.). The development of an enhanced version of SUD is envisaged using for instance an object oriented database (O2 ?), the MOTIF user interface and AVS. Such a new system would allow the user to build interactively (graphically) the detector, interact with GEANT and eventually visualise the simulated event. Of course the possibility of integrating existing or forthcoming GEANT developments (in particular, its user interface) is seriously being considered.

IV. ACTIVITIES FORESEEN FOR 1993/1994

The ideas and results presented herein show that Monte Carlo simulations are indeed a multitask activity, where the diversity of problems to be experienced, and hopefully solved, is practically unlimited. The efforts should concentrate on the following directions.

First of all, on new Physics inputs. Second, to provide the most reliable predictions up to the highest energy one can realistically foresee for the next generation of supercolliders. Special emphasis should be given to an extensive study of SUSY particle production and detection (missing energy signatures, etc.).

As far as the development of software tools is concerned, it is necessary to cope with the ever growing complexity of the Physics phenomena one will have to analyse in the future. In addition to the above graphics development, particular care will be devoted to the problem of speed in Monte Carlo simulation computing.

	PYTHIA		QGSM	
$\sqrt{s}$ (TeV)	N_{ch}	D	N_{ch}	D
0.062	12.5	6.5	12.4	6.4
0.63	24.9	16.5	32.5	19.9
1.8	34.3	24.4	45.8	29.8
16	60.1	45.3	83.1	63.4
40	73.6	58.5	107.0	87.0
200	103.0	87.1	159.0	139.0

Table 1

The mean multiplicities $<N_{ch}>$ and dispersions $D = \sqrt{<N_{ch}^2> - <N_{ch}>^2}$ in PYTHIA (with EHLQ1 [26] structure functions) and in QGSM.

Cross-sections (in pb) for Higgs production:

$\sqrt{s}$ = 16 TeV	M_H=500 GeV	M_H=750 GeV	M_H=1000 GeV
$q\bar{q}$	6.563×10^{-5}	2.553×10^{-5}	9.791×10^{-6}
gg	8.707×10^{-4}	1.254×10^{-4}	3.231×10^{-5}
$Z^0 Z^0$	8.535×10^{-5}	3.059×10^{-5}	1.200×10^{-5}
W^+W^-	1.802×10^{-4}	6.584×10^{-5}	2.650×10^{-5}

$\sqrt{s}$ = 40 TeV	M_H=500 GeV	M_H=750 GeV	M_H=1000 GeV
$q\bar{q}$	5.189×10^{-4}	2.645×10^{-4}	1.172×10^{-4}
gg	4.973×10^{-3}	8.887×10^{-4}	2.416×10^{-4}
$Z^0 Z^0$	4.653×10^{-4}	2.161×10^{-4}	1.093×10^{-4}
W^+W^-	1.034×10^{-3}	4.780×10^{-4}	2.220×10^{-4}

$\sqrt{s}$ = 200 TeV	M_H=500 GeV	M_H=750 GeV	M_H=1000 GeV
$q\bar{q}$	7.182×10^{-3}	4.524×10^{-3}	1.984×10^{-3}
gg	5.623×10^{-2}	1.215×10^{-2}	3.746×10^{-3}
$Z^0 Z^0$	5.064×10^{-3}	2.722×10^{-3}	1.512×10^{-3}
W^+W^-	1.044×10^{-2}	5.617×10^{-3}	1.134×10^{-3}

Cross-sections (in pb) for Background events:

	$\sqrt{s}$=16 TeV	$\sqrt{s}$=40 TeV	$\sqrt{s}$=200 TeV
$q\bar{q}$	1.492×10^{-2}	3.865×10^{-2}	1.356×10^{-1}
gg	$0.266 \times \sigma_{q\bar{q}}$	$0.450 \times \sigma_{q\bar{q}}$	$\sigma_{q\bar{q}}$

Table 2

Cross-sections for $H^0 \to Z^0 Z^0 \to \mu\mu\mu\mu$ production and for $Z^0 Z^0 \to \mu\mu\mu\mu$ background production in pp interactions at different $\sqrt{s}$ energies and Higgs masses, as derived in PYTHIA and in [34].

REFERENCES

1 F. Anselmo, L. Cifarelli, E. Eskut and Yu. M. Shabelski, preprint EMCSC/ELN 92-01, 15 August 1992.

2 A.B. Kaidalov and K.A. Ter-Martirosyan, Yad. Fiz. 39 (1984) 1545; 40 (1984) 211. A.B. Kaidalov and O.I. Piskunova, Yad. Fiz. 41 (1985) 1278. Yu. M. Shabelski, Yad. Fiz. 44 (1986) 186. Yu. M. Shabelski, Z. Phys. C 38 (1988) 569.

3 A. Capella et al., Phys. Lett. B81 (1979) 68. H. Minakata, Phys. Rev. D20 (1979) 1656. G. Cohen-Tannoudji et al., Phys. Rev. D19 (1979) 3397; D21 (1980) 2699.

4 B. Andersson et al., Phys. Rep. 97 (1983) 31.

5 T. Sjöstrand, Comp. Phys. Comm. 39 (1986) 347. T. Sjöstrand and M. Bengtsson, Comp. Phys. Comm. 43 (1987) 367. H.U. Bengtsson and T. Sjöstrand, Comp. Phys. Comm. 46 (1987) 43. T. Sjöstrand and M. van Zijl, Phys. Rev. D36 (197) 2019. T. Sjöstrand, preprint CERN-TH.6488/92, May 1992.

6 L. Cifarelli, E. Eskut and Yu. M. Shabelski, preprint EMCSC/ELN 92-02, 30 August 1992.

7 D. Decamp et al. (ALEPH Collaboration), Phys. Lett. B 236 (1990) 233; Phys. Lett B 241 (1990) 141. P.D. Acton et al. (OPAL Collaboration), Phys. Lett. B 236 (1990) 224. M. Dittmar, KEK seminar, May 1990.

8 F. Anselmo, E. Blanco, G. Brugnola, L. Cifarelli and D. Hatzifotiadou, "Higgs Search at Future Supercolliders", preprint in preparation.

9 F. Block et al., "Neural Networks for Higgs Search", preprint in preparation.

10 L. Lönnblad, C. Peterson, T. Rögnvaldsson, preprint LU TP 91-18, August 1991.

11 F. Anselmo, L. Cifarelli, A. Peterman and A. Zichichi, Il Nuovo Cimento vol.104 A, N. 12 (1991) 1817.

12 F. Anselmo, L. Cifarelli, A. Peterman and A. Zichichi, preprint CERN/LAA/MSL/91-026, December 1991, to appear on "Il Nuovo Cimento".

13 F. Anselmo, L. Cifarelli, A. Peterman and A. Zichichi, Il Nuovo Cimento vol.105 A, N. 4 (1992) 581.

14 F. Anselmo, L. Cifarelli, A. Peterman and A. Zichichi, preprint CERN-PPE/92-103, 22 June 1992, to appear on "Il Nuovo Cimento".

15 F. Anselmo, L. Cifarelli, A. Peterman and A. Zichichi, preprint CERN-TH.6543/92 June 1992, to appear on "Il Nuovo Cimento".

16 F. Anselmo, L. Cifarelli and A. Zichichi, preprint CERN/LAA/MSL/92-011 July 1992, to appear on "Il Nuovo Cimento".

17 F. Anselmo, L. Cifarelli and A. Zichichi, preprint CERN-PPE/92-122, 4 July 1992, to appear on "Il Nuovo Cimento".

18 R. Brun, F. Bruyant, M. Maire, A.C. McPherson, P. Zanarini, "GEANT 3", CERN DD/EE/84-1.

19 F. Anselmo, E. Barberio, G. Bruni, P. Bruni, L. Cifarelli, O. Di Rosa, G. Iacobucci, G. La Commare, M. Marino, R. Nania and A. Zichichi, Particle World (Communications in Subatomic Physics) vol.2, No.4 (1991) 108.

20 ADAMO Notes, the ALEPH Collaboration, March 28, 1988. M.G. Green, RHBNC 89-01 and CERN-DD/US/131, March 15, 1989. The ADAMO package has recently been included in the CERN Program Library.

21 J. Alberty, F.Anselmo, A. Bassi, G. Bruni, P. Bruni, L. Cifarelli, O. Di Rosa, D. Hatzifotiadou, G. Iacobucci, G. La Commare, M. Marino and R. Nania, "FMC User's Guide", CERN/LAA-MSL/90-06. L. Cifarelli, G. La Commare and M. Marino, preprint CERN/ECP 91-20, 24 September 1991 and Il Nuovo Cimento 105 A, N.4 (1992) 597.

22 "The LAA Project", CERN-LAA/89-1, p. 77 and p. 295.

23 J. Alberty et al., "Monte Carlo simulation for the LAA Detector", in Proceedings of the 14th Workshop of the INFN Eloisatron Project on "Perspectives for New Detectors in Future Supercolliders", Erice, Italy, 17-24 October 1989 (eds. L. Cifarelli, R. Wigmans and T. Ypsilantis, World Scientific, Singapore), p. 160. G. Anzivino et al. "A general definition for a HEP apparatus based on the ADAMO package in the framework of the GEANT Monte Carlo program", in Proceedings of the 1st International Workshop on Software Engineering, Artificial Intelligence and Expert System in High Energy Physics: "New Computing Techniques in Physics Research", Lyon Villeurbanne, France, 19-24 March 1990 (eds. D. Perret-Gallix and W. Wojcik, Editions du Centre National de la Recherche Scientifique, Paris), p. 143. A. Bassi, G. Bruni, L. Cifarelli, G. Iacobucci, G. La Commare, M. Marino and R. Nania, preprint CERN/ECP 91-18, 23 September 1991. A. Bassi, G. Bruni, L. Cifarelli, A. Contin, G. Iacobucci, G. La Commare, M. Marino and R. Nania, "SUD: An Advanced Set-Up Descriptor for Complex Multi-TeV Experiments", to appear on "Il Nuovo Cimento".

24 R. Brun, P. Zanarini, "KUIP Users Guide", CERN-DD I202, February 26 1988.

25 G. La Commare, B. van Eijk, M. Marino, preprint CERN/ECP 91-19, 21 November 1991.

26 E. Eichten, I. Hinchliffe, K. Lane and C. Quigg, Rev. of Mod. Phys., Vol. 56, No. 4 (1984) 579. Erratum: Rev. of Mod. Phys., Vol. 58, No. 4 (1986) 1065.

27 F. Abe et al., preprint FERMILAB-Pub-89/201-E (1989). UA5 Coll., G.J. Alner et al., Phys. Rep. 154 (1987) 247; Phys. Lett. 160B (1985) 193.

28 G. Bari et al., Il Nuovo Cimento Vol. 104 A (1991) 571.

29 J.G. Morfin and W.-K. Tung, preprint FERMILAB-Pub-90/74 (1990).

30 M. Gluck, E. Reya and A. Vogt, Z. Phys. C48 (1990) 471.

31 G. Marchesini and B.R. Webber, Nucl. Phys. B130 (1988) 571.

32 F.E. Paige, S.D. Protopopescu, preprints: BNL-29777, October 1981; BNL-31987, September 1982; BNL-37271, August 1985; BNL-38034, March 1986; BNL-38774, September 1986.

33 A. Ali and B. van Eijk, in Proceedings of the 5th Topical Workshop on "Proton-Antiproton Collider Physics", St. Vincent, Aosta, Italy, 1985. B. van Eijk, preprint CERN-EP85-121. A. Ali, B. van Eijk and I. ten Have, CERN-TH.4523/86, Nucl. Phys. B292 (1987) 1.

34 L. Cifarelli, "Super Monte Carlo Simulations at 16, 40, 200 TeV" in Proceedings of the 28th Course of the International School of Subnuclear Physics, Erice, Italy, 16-24 July 1990: "Physics up to 200 TeV" (ed. A. Zichichi, Plenum Press, New York-London), p. 409.

35 G. Xexeo, G. La Commare and J. Souza, "The CAB Database", in Proceedings of the 14th Workshop of the INFN Eloisatron Project on "Data Structures for Particle Physics Experiments: Evolution or Revolution?", Erice, Italy, 11-18 November 1990 (eds. R. Brun, P. Kuns and P. Palazzi, World Scientific Singapore), p. 77. G. Xexeo, G. La Commare and J. Souza, "CAB: The Cosmos Application Builder", in Proceedings of "Computing in High Energy Physics", Tsukuba, Japan, 11-15 March 1991, (eds. Y. Watase, F. Abe, Universal Academy Press, Inc.-Tokyo), p. 359.

36 C. Maidantchik, A.R.C. da Rocha, G. Xexeo, G. La Commare and J. Souza, "SIM: A Software Information Manager" in Proceedings of "Computing in High Energy Physics", Tsukuba, Japan, 11-15 March 1991, (eds. Y. Watase, F. Abe, Universal Academy Press, Inc.-Tokyo), p. 335.

FIGURE CAPTIONS

Figure 1 Feynman-x distributions of π^+(a), K^-(b) and p(c) hadrons produced in pp collisions at $\sqrt{s}$= 16 TeV in PYTHIA (black points) and QGSM (open points). EHLQ1 (set 1) [26] structure functions are used in PYTHIA. We use the variable $x_E/\sigma_{in} \cdot d\sigma/xF$ (where $x_F=2p_L/\sqrt{s}$, $x_E=2E/\sqrt{s}$, σ_{in}=total inelastic cross-section) since this is not affected by any kinematical singularity for $E \simeq x_F \simeq 0$.

Figure 2 Same as figure 1, for pp collisions at $\sqrt{s}$ = 40 TeV.

Figure 3 Same as figure 1, for π^-(a), K^-(b), p(c) and $\bar{p}$(d) production in pp interactions at $\sqrt{s}$ = 200 TeV.

Figure 4 Charged particle multiplicity distributions in $p\bar{p}$ collisions at $\sqrt{s}$ = 540 GeV [27] (a), compared with the predictions from PYTHIA (black points), using EHLQ1 [26] structure functions, and QGSM (open points). The same predictions are derived for pp collisions at $\sqrt{s}$ = 16 TeV (b).

Figure 5 x_F-distributions of outgoing protons in pp collisions at $\sqrt{s}$ = 62 GeV, 1.8 TeV and 200 TeV, as indicated, derived with QGSM (a) and PYTHIA (b). EHLQ1 [26] structure functions are used.

Figure 6 Inclusive x_F-spectrum of Λ_c^+ produced in pp collisions at $\sqrt{s}$ = 62 GeV [28]. The QGSM and PYTHIA predictions (using EHLQ1 [26], MT2 [29], GRV2 [30] structure functions) are shown as black and open points respectively, as indicated.

Figure 7 PYTHIA (with EHLQ1 [26] structure functions and variant K2 of K-factor [5]) and QGSM predictions for the x_F-distributions of charm (a) and beauty (b) mesons and baryons produced in $p\bar{p}$ interactions at $\sqrt{s}$ = 630 GeV. The PYTHIA results are shown as different kinds of points, the QGSM ones as different kind of curves, as indicated. The distributions refer to the outgoing p hemisphere.

Figure 8 PYTHIA predictions (a) (with EHLQ1 [26] structure functions and variant K2 of K-factor [5]) for the x_F-distributions of strange, charmed and beautiful baryons in pp interactions at $\sqrt{s}$ = 630 GeV, and QGSM predictions (b) at $\sqrt{s}$ = 630 GeV (open points) and $\sqrt{s}$ = 200 TeV (black points).

Figure 9 PYTHIA predictions for the charged particle multiplicity distribution in pp interactions at $\sqrt{s} = 40$ TeV (a) and 200 TeV (b). Three different sets of structure functions are used: one "old" set (EHLQ1 [26]) and two "new" ones (MT2 [29] and GRV2 [30]). With the "new" sets, the power increase of the gluon distribution at very small x, i.e. very high $\sqrt{s}$, produces very high multiplicities due to many multiparton interactions. This effect is absent in the "old" set.

Figure 10 Four muon invariant mass spectra before and after cuts ($|y_\mu| < 3$ and $p_{t\mu} > 60$ GeV/c, for each μ), as obtained in pp interactions for Higgs production at $\sqrt{s} = 16$, 40 and 200 TeV, with $m_H = 500$ GeV.

Figure 11 Same as figure 10, for $m_H = 750$ GeV.

Figure 12 Same as figure 10, for $m_H = 1$ TeV.

Figure 13 Higgs purity versus efficiency as obtained with NN analysis for Higgs production at $\sqrt{s} = 16$, 40 and 200 TeV, with $m_H = 750$ GeV.

Figure 14 Summary of our studies on the effective threshold for Supersymmetry (SUSY) breaking [11-17]. A correct treatment of the evolution of the α_1, α_2, α_3 couplings and of all particle and sparticle masses (in particular of the gaugino masses) is made; a detailed spectrum of light sparticles is introduced at the level of the light threshold where SUSY [SU(3)×SU(2)×U(1)] breaks into SU(3)×SU(2)×U(1); a smooth heavy threshold is considered just below the Grand Unification point (E_{GUT}) where SUSY [SU(5)] breaks into SUSY [SU(3)×SU(2)×U(1)]. Taking $\pm 2\sigma$ errors for the experimental inputs ($1/\alpha_{em}$, α_s, $\sin^2\theta_W$ at m_{Z^0}), the conclusion is that the SUSY breaking threshold could be as low as the Z^0 mass.

Figure 15 Two examples of SUSY particle mass spectra as obtained in [14]. The lightest sparticle could be either the W-ino (with $m_{\tilde{W}} \simeq 100$ GeV) or the higgsino (with $m_{\tilde{H}} \simeq 200$ GeV).

Figure 16 Example of Higgs event produced in pp collisions at $\sqrt{s} = 40$ TeV in the "LAA test detector". The process is $gg \to H^0 \to Z^0 Z^0 \to \mu\mu\mu\mu$, with $m_H = 750$ GeV and $p_{tZ^0} > 80$ GeV (for each Z^0). The total event multiplicity is ~550. Only tracks with $p > 0.1$ GeV are displayed.

Figure 17 The Entity (panel) - Relationship (arrow) diagram of the MEGA database showing how the output of an event generator is organised via ADAMO. The various attributes of each entity are self-explanatory.

Figure 18 The structure of the FMC (Full Monte Carlo Chain) showing how the various databases (MEGA for event generator output, PDKDB for particle properties and SUD for detector description) are interfaced with the most widely used event generators, i.e. LUND (PYTHIA) [5], HERWIG [31], ISAJET [32], EUROJET [33], and with the well-known GEANT tracking program [18].

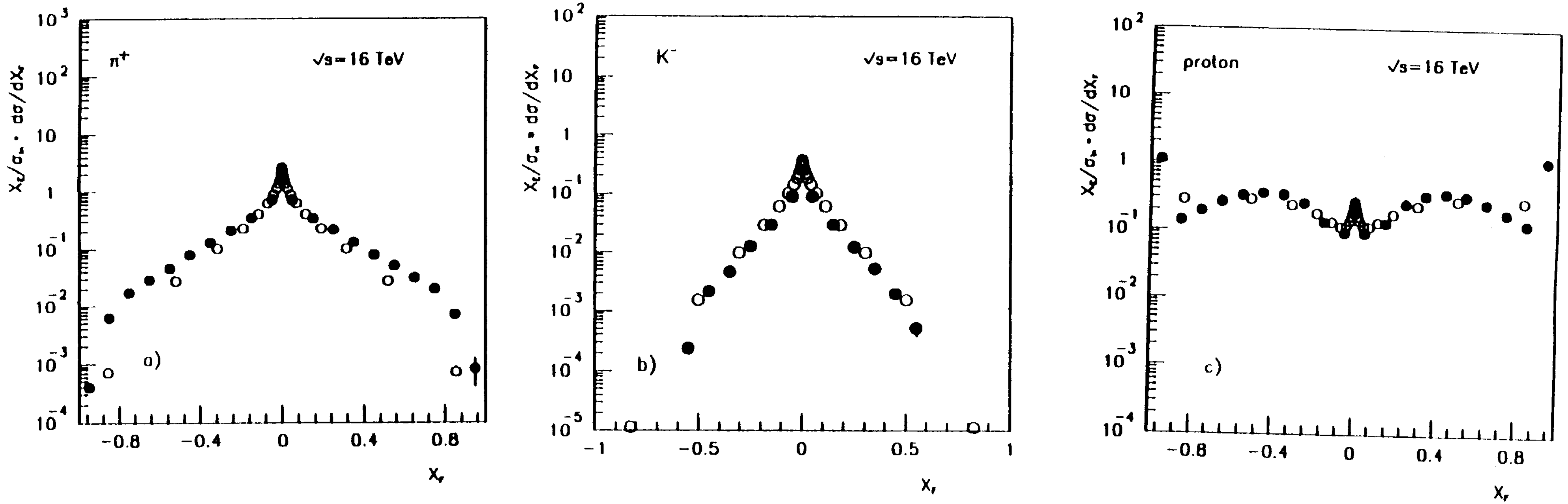

Figure 1

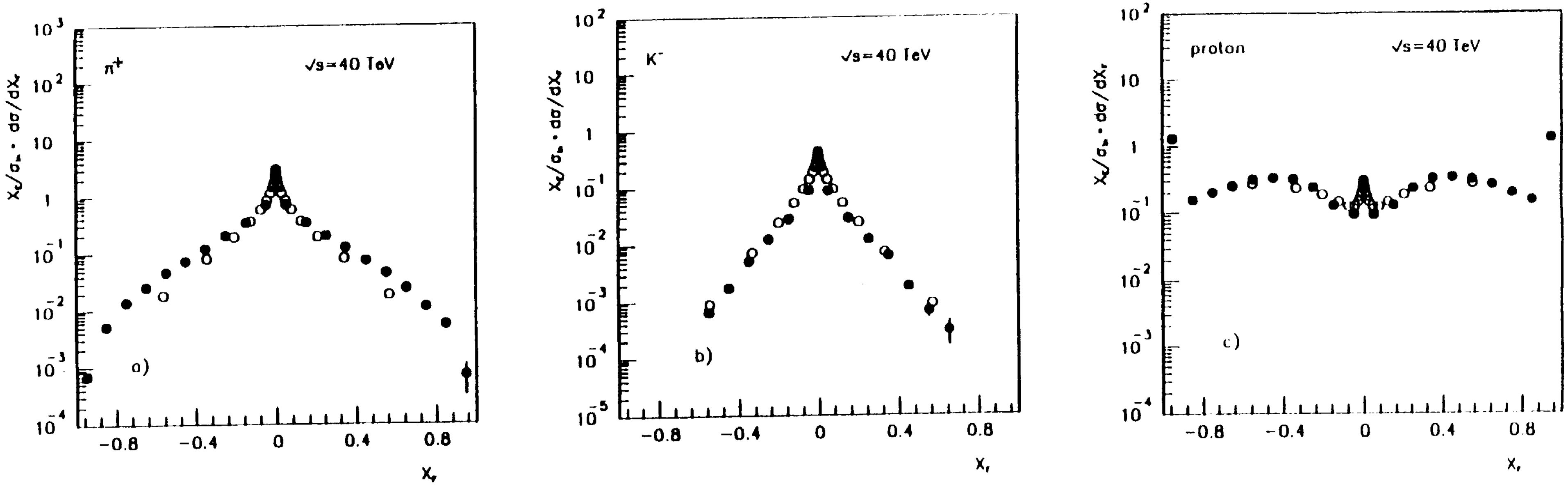

π+
√s=40 TeV
a)
K-
√s=40 TeV
b)
proton
√s=40 TeV
c)
$x_r/\sigma_{in} \cdot d\sigma/dx_r$
x_r

Figure 2

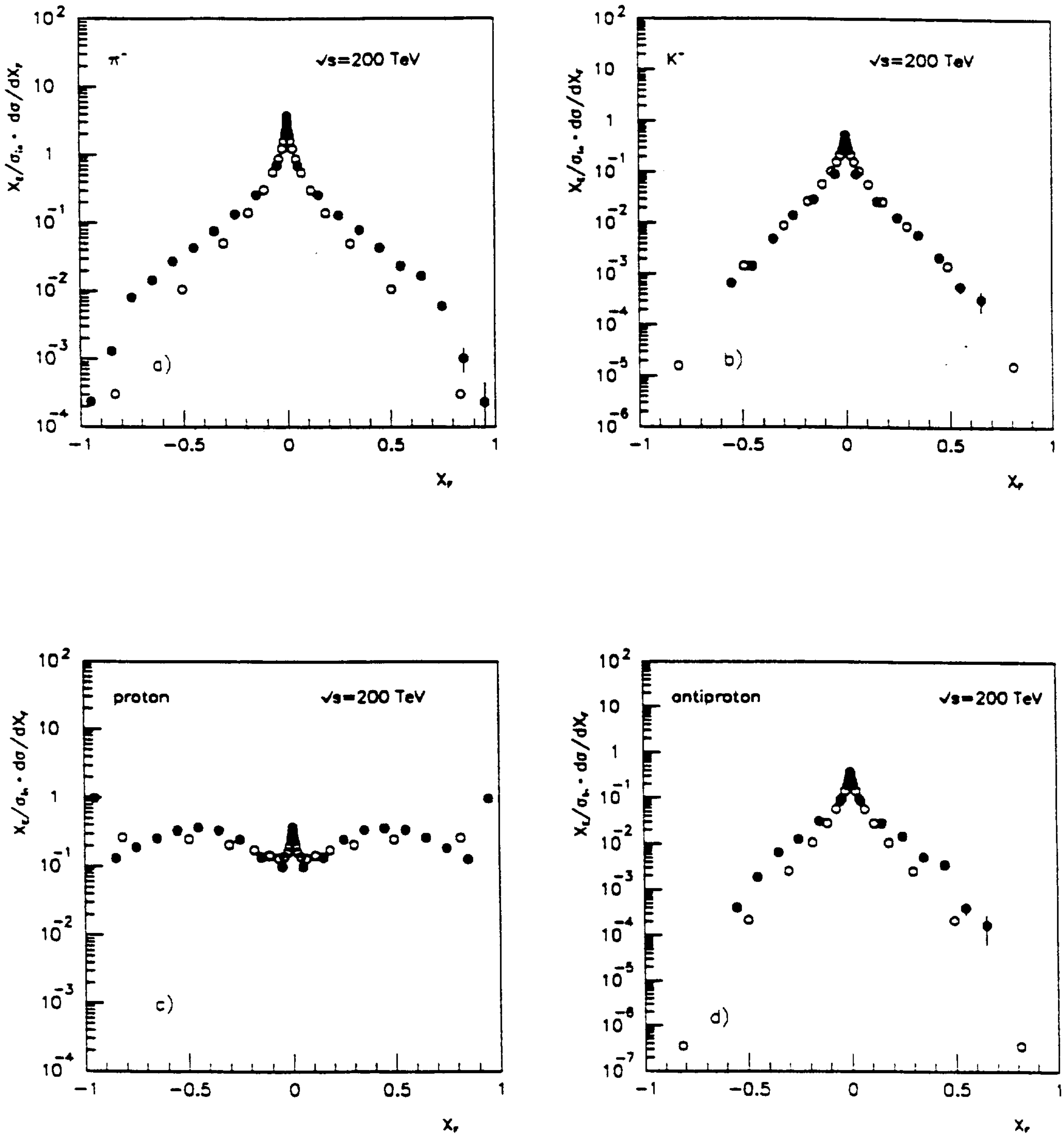

π⁻
√s=200 TeV
a)
K⁻
√s=200 TeV
b)
proton
√s=200 TeV
c)
antiproton
√s=200 TeV
d)
X_F

Figure 3

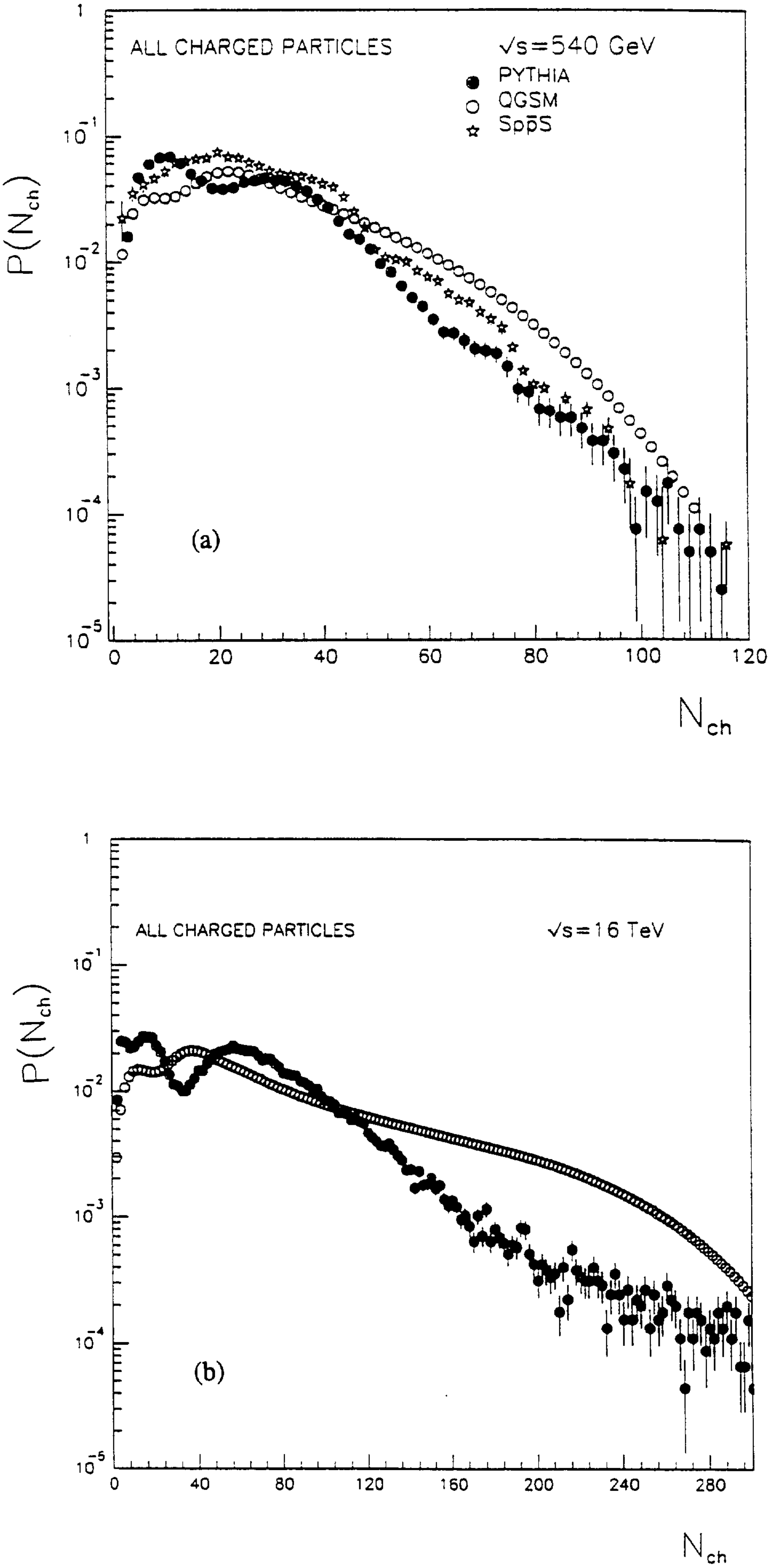
ALL CHARGED PARTICLES
√s=540 GeV
PYTHIA
QGSM
Sp$\bar{p}$S
(a)
P(N_ch)
N_ch
ALL CHARGED PARTICLES
√s=16 TeV
(b)
P(N_ch)
N_ch

Figure 4

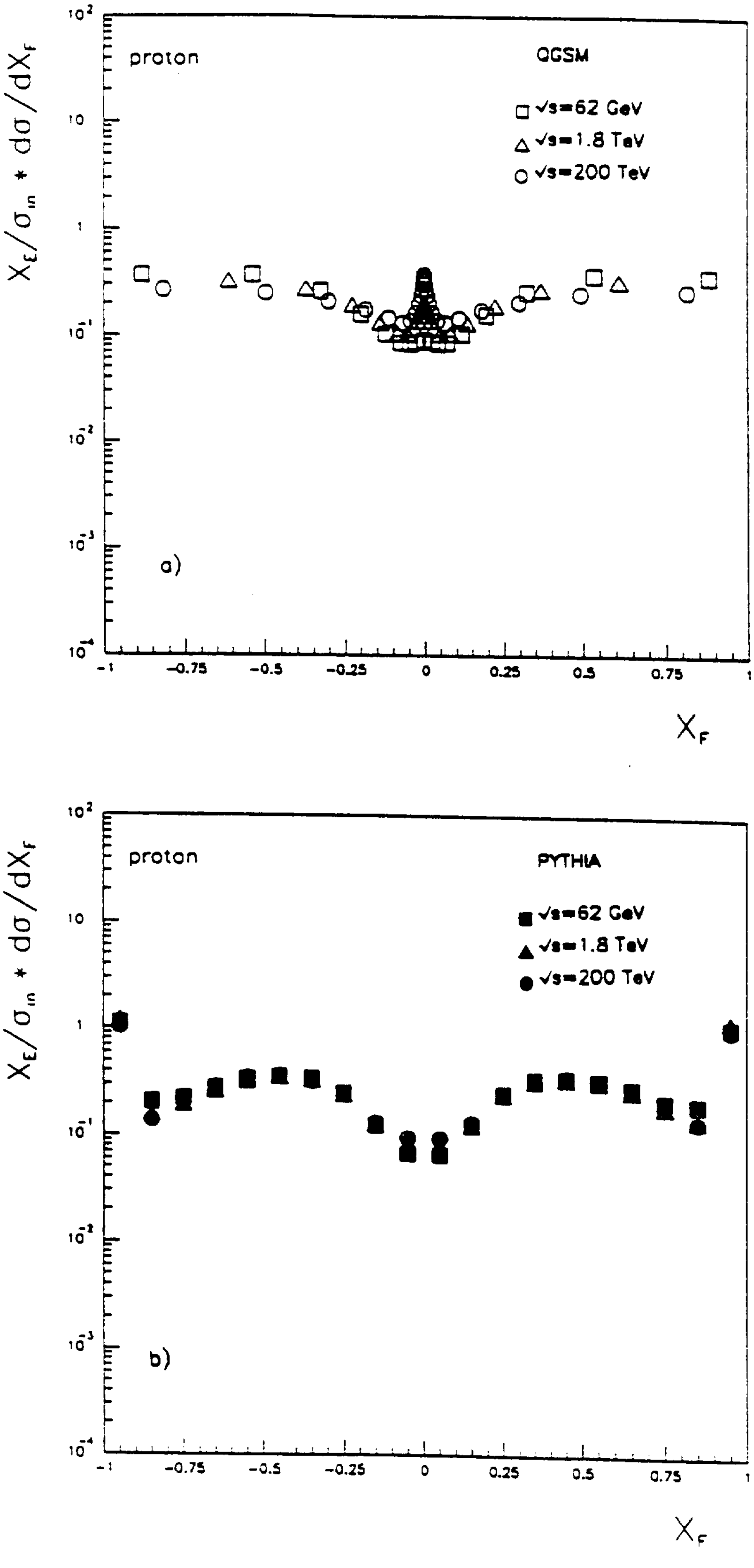

proton
QGSM
√s=62 GeV
√s=1.8 TeV
√s=200 TeV
a)
$X_F/\sigma_{in} * d\sigma/dX_F$
X_F
proton
PYTHIA
√s=62 GeV
√s=1.8 TeV
√s=200 TeV
b)
$X_F/\sigma_{in} * d\sigma/dX_F$
X_F

Figure 5

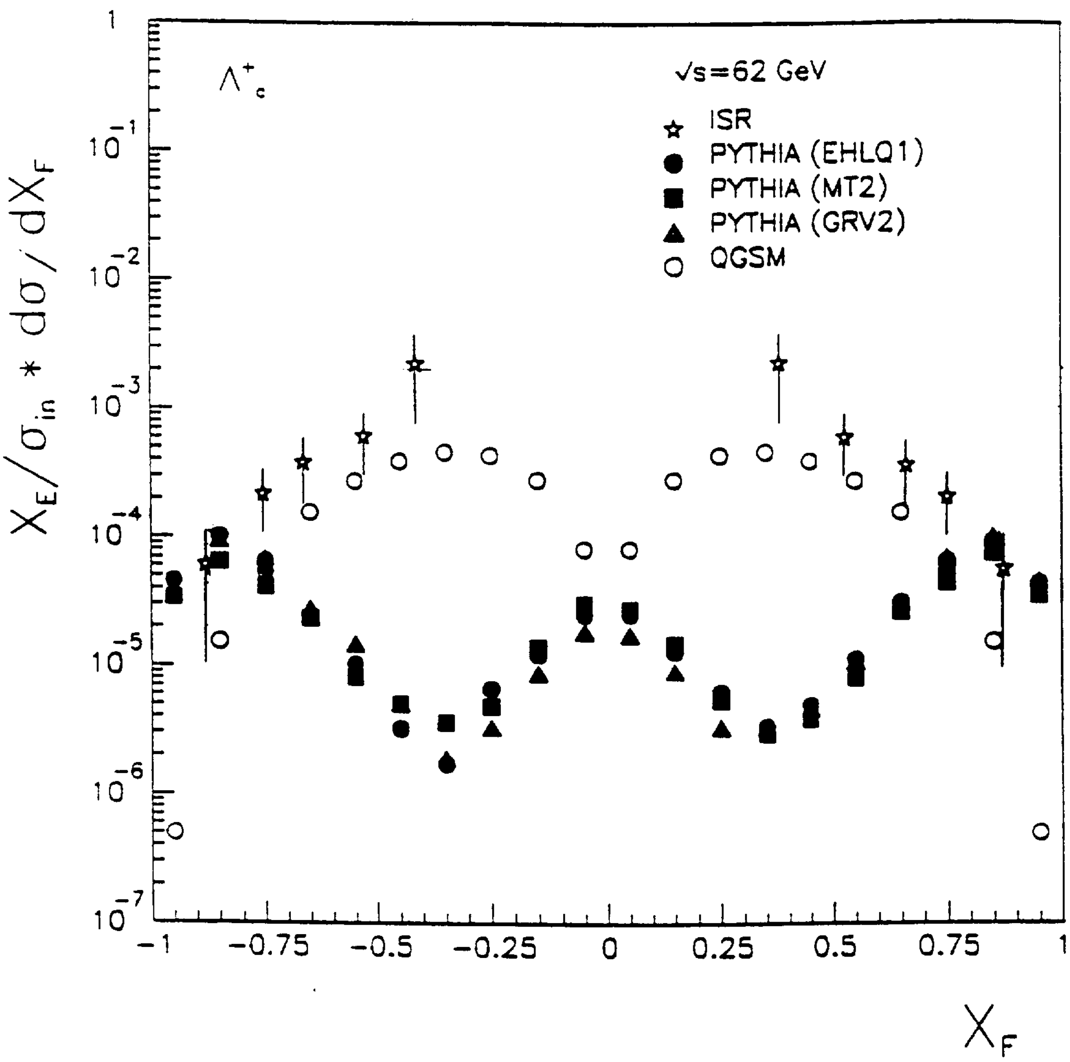

Λ^+_c
$\sqrt{s}$=62 GeV
ISR
PYTHIA (EHLQ1)
PYTHIA (MT2)
PYTHIA (GRV2)
QGSM
$X_E/\sigma_{in} * d\sigma/dX_F$
X_F

Figure 6

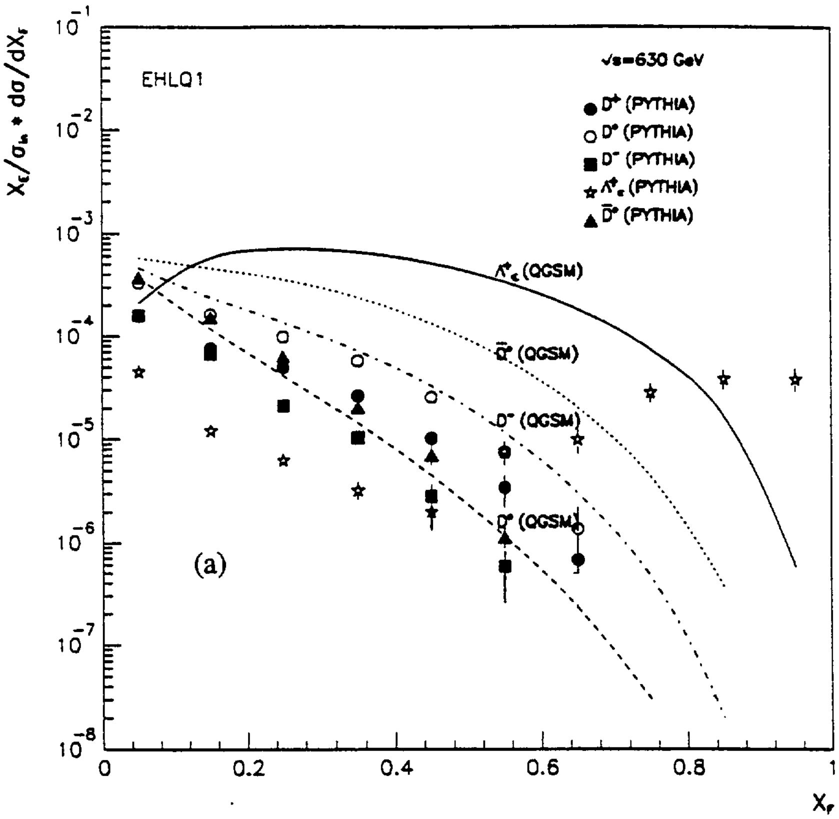
EHLQ1
√s=630 GeV
D+ (PYTHIA)
D0 (PYTHIA)
D- (PYTHIA)
Λ+c (PYTHIA)
D̄0 (PYTHIA)
Λ+c (QGSM)
D̄0 (QGSM)
D- (QGSM)
D0 (QGSM)
(a)
Xf
Xf/σin * dσ/dXf

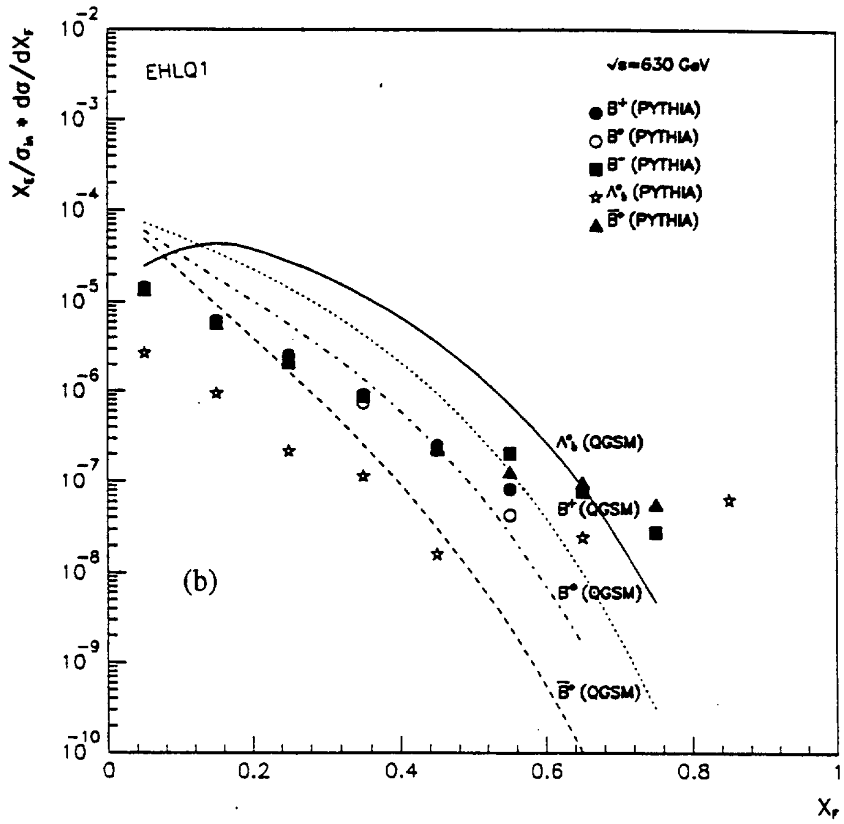
EHLQ1
√s=630 GeV
B+ (PYTHIA)
B0 (PYTHIA)
B- (PYTHIA)
Λ0b (PYTHIA)
B̄0 (PYTHIA)
Λ0b (QGSM)
B+ (QGSM)
B0 (QGSM)
B̄0 (QGSM)
(b)
Xf
Xf/σin * dσ/dXf

Figure 7

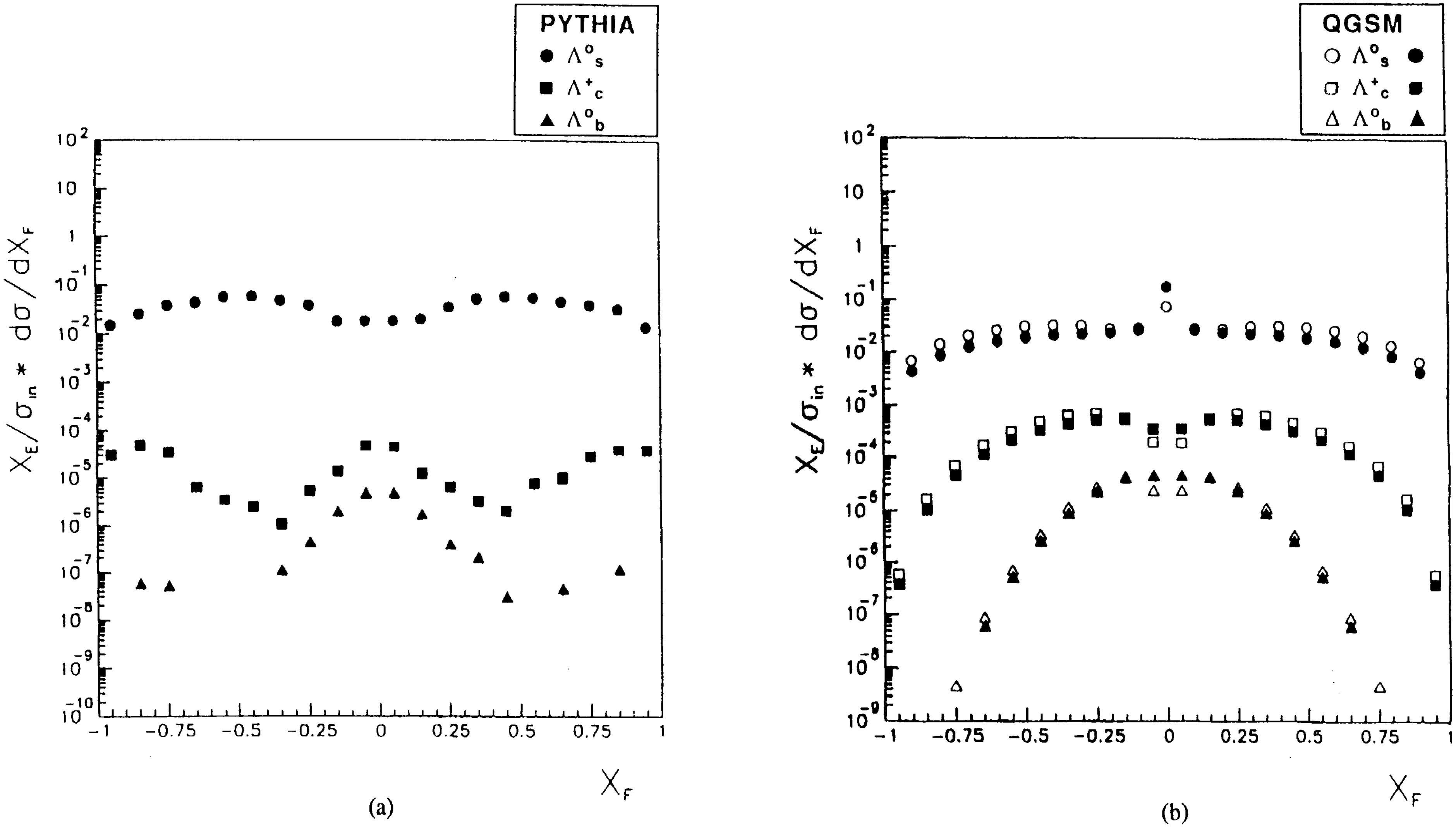

Figure 8

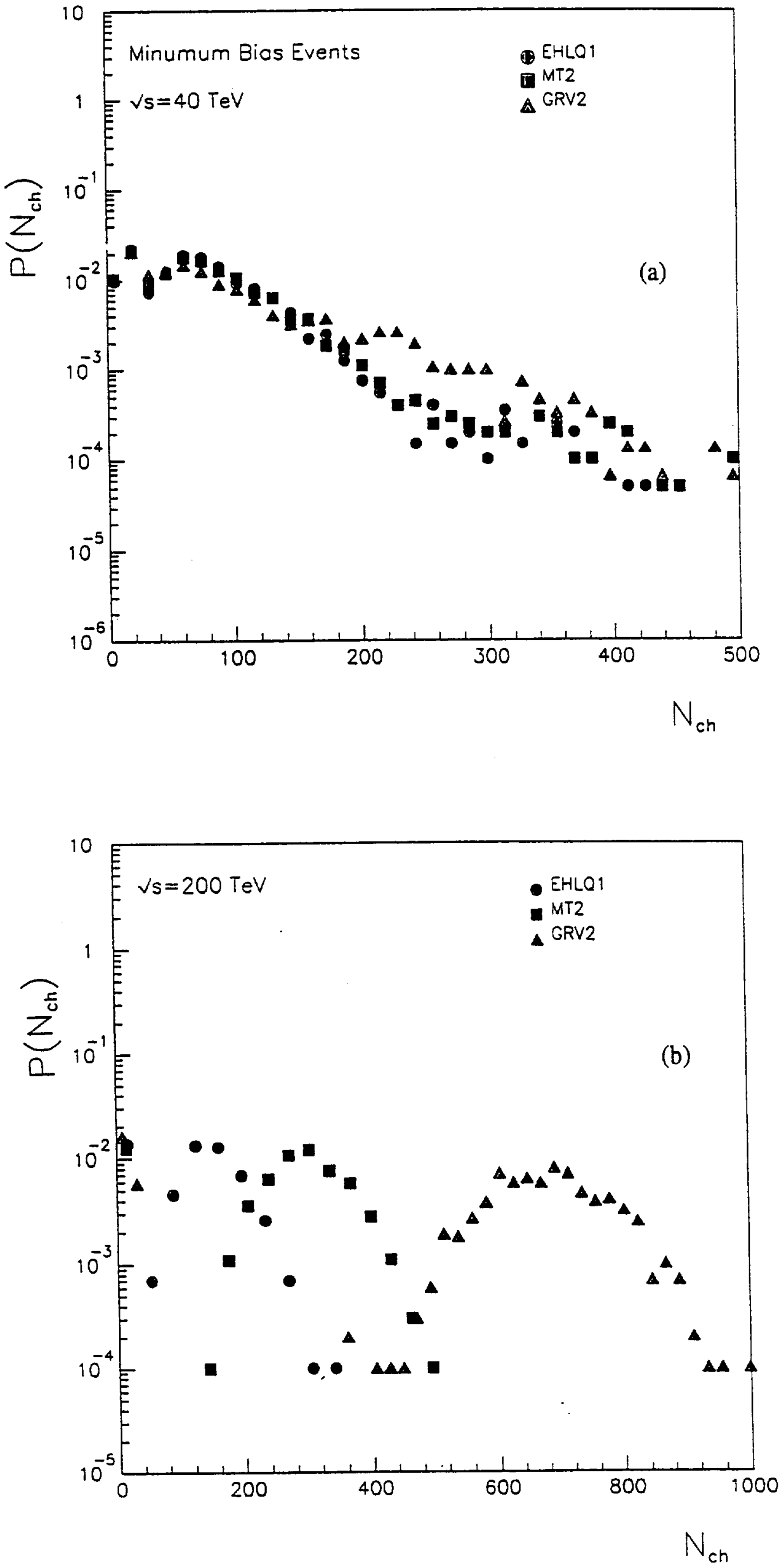

Minumum Bias Events
√s=40 TeV
EHLQ1
MT2
GRV2
(a)
P(N_ch)
N_ch
√s=200 TeV
EHLQ1
MT2
GRV2
(b)
P(N_ch)
N_ch

Figure 9

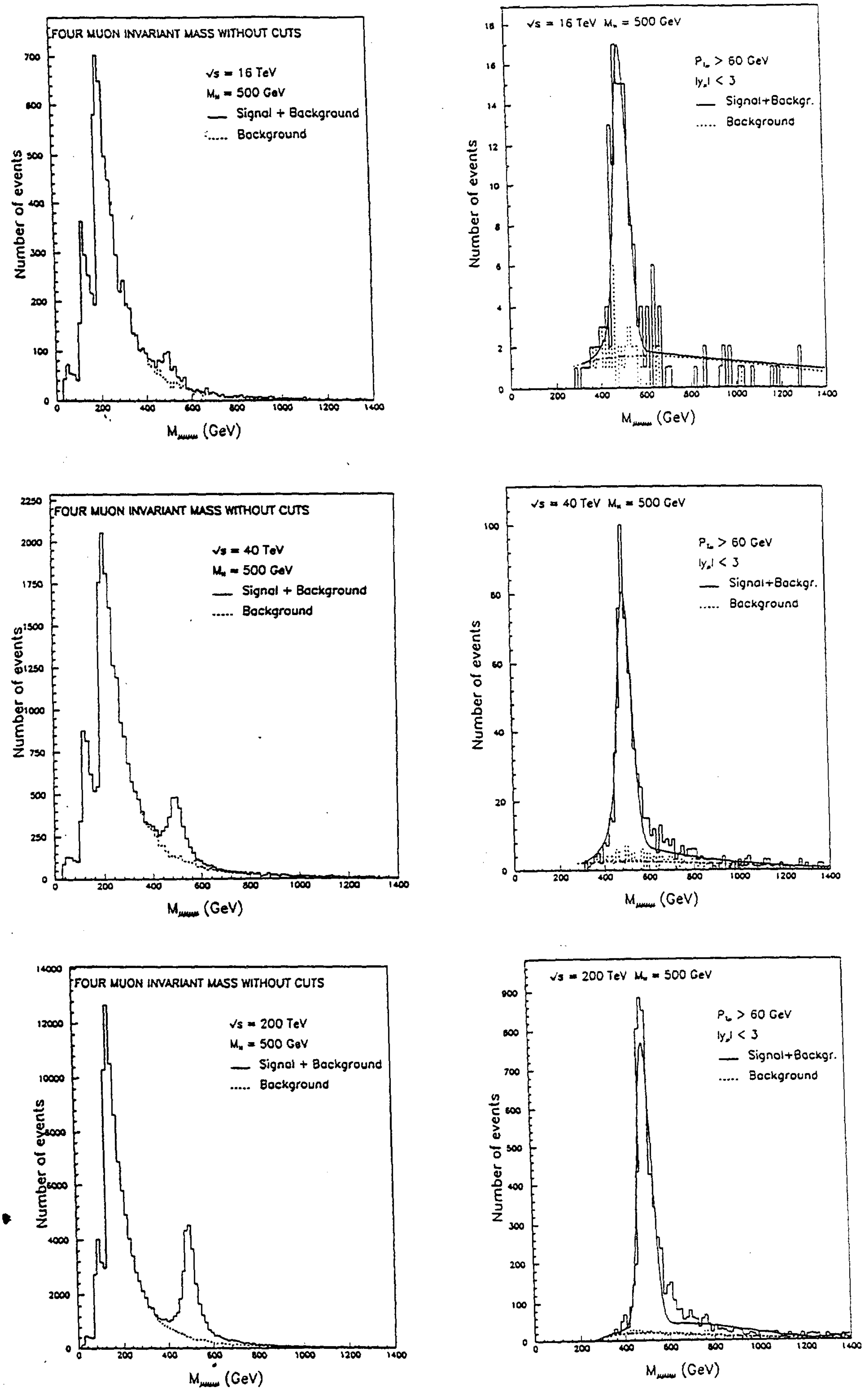

FOUR MUON INVARIANT MASS WITHOUT CUTS
√s = 16 TeV
M_H = 500 GeV
Signal + Background
Background
Number of events
M_μμμμ (GeV)
√s = 16 TeV M_H = 500 GeV
P_tμ > 60 GeV
|y_μ| < 3
Signal+Backgr.
Background
Number of events
M_μμμμ (GeV)
FOUR MUON INVARIANT MASS WITHOUT CUTS
√s = 40 TeV
M_H = 500 GeV
Signal + Background
Background
Number of events
M_μμμμ (GeV)
√s = 40 TeV M_H = 500 GeV
P_tμ > 60 GeV
|y_μ| < 3
Signal+Backgr.
Background
Number of events
M_μμμμ (GeV)
FOUR MUON INVARIANT MASS WITHOUT CUTS
√s = 200 TeV
M_H = 500 GeV
Signal + Background
Background
Number of events
M_μμμμ (GeV)
√s = 200 TeV M_H = 500 GeV
P_tμ > 60 GeV
|y_μ| < 3
Signal+Backgr.
Background
Number of events
M_μμμμ (GeV)

Figure 10

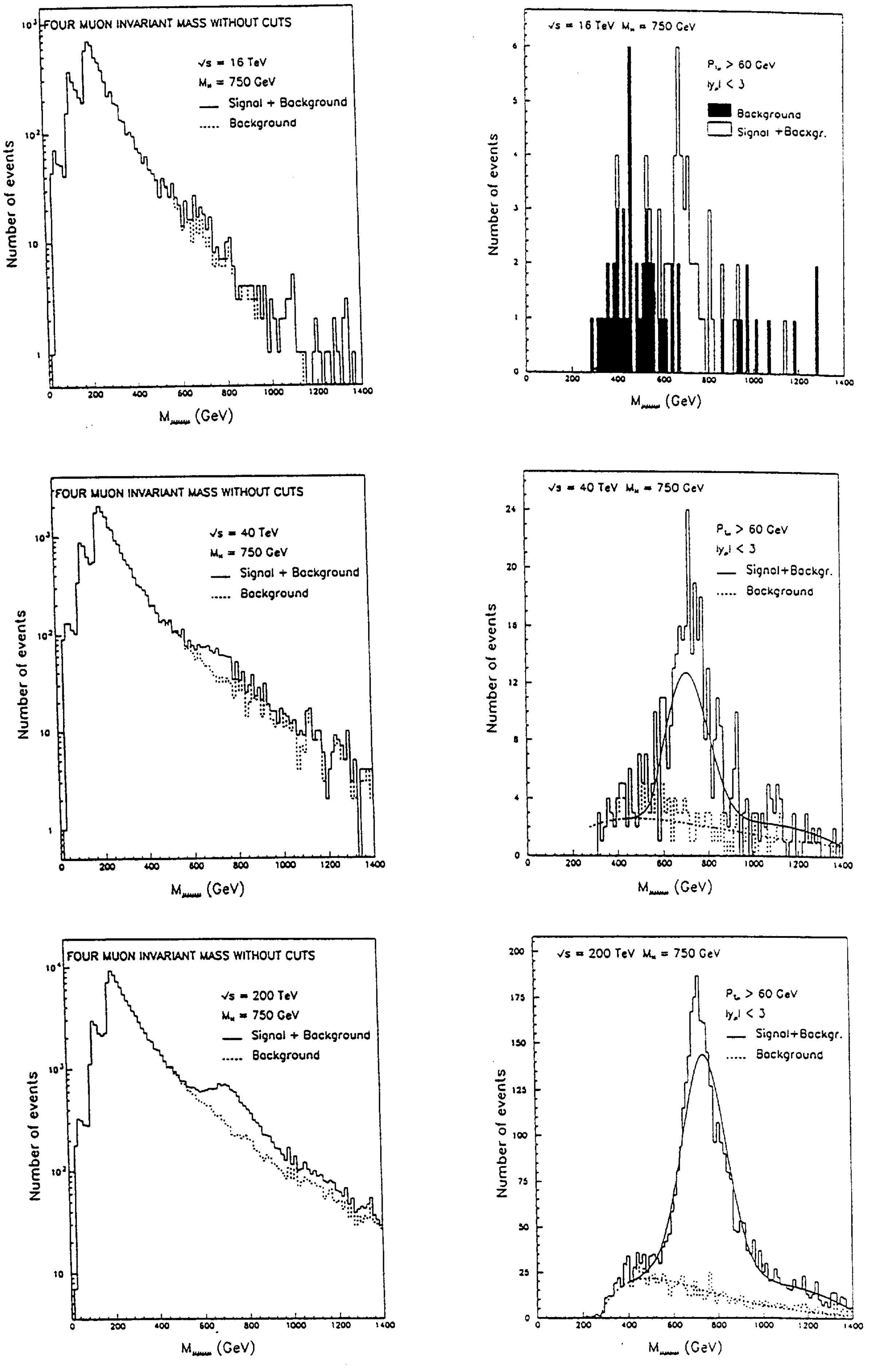

FOUR MUON INVARIANT MASS WITHOUT CUTS
√s = 16 TeV
M_H = 750 GeV
Signal + Background
Background
Number of events
$M_{\mu\mu\mu\mu}$ (GeV)
√s = 16 TeV M_H = 750 GeV
$P_{t\mu}$ > 60 GeV
$|y_\mu|$ < 3
Background
Signal +Backgr.
Number of events
$M_{\mu\mu\mu\mu}$ (GeV)
FOUR MUON INVARIANT MASS WITHOUT CUTS
√s = 40 TeV
M_H = 750 GeV
Signal + Background
Background
Number of events
$M_{\mu\mu\mu\mu}$ (GeV)
√s = 40 TeV M_H = 750 GeV
$P_{t\mu}$ > 60 GeV
$|y_\mu|$ < 3
Signal+Backgr.
Background
Number of events
$M_{\mu\mu\mu\mu}$ (GeV)
FOUR MUON INVARIANT MASS WITHOUT CUTS
√s = 200 TeV
M_H = 750 GeV
Signal + Background
Background
Number of events
$M_{\mu\mu\mu\mu}$ (GeV)
√s = 200 TeV M_H = 750 GeV
$P_{t\mu}$ > 60 GeV
$|y_\mu|$ < 3
Signal+Backgr.
Background
Number of events
$M_{\mu\mu\mu\mu}$ (GeV)

Figure 11

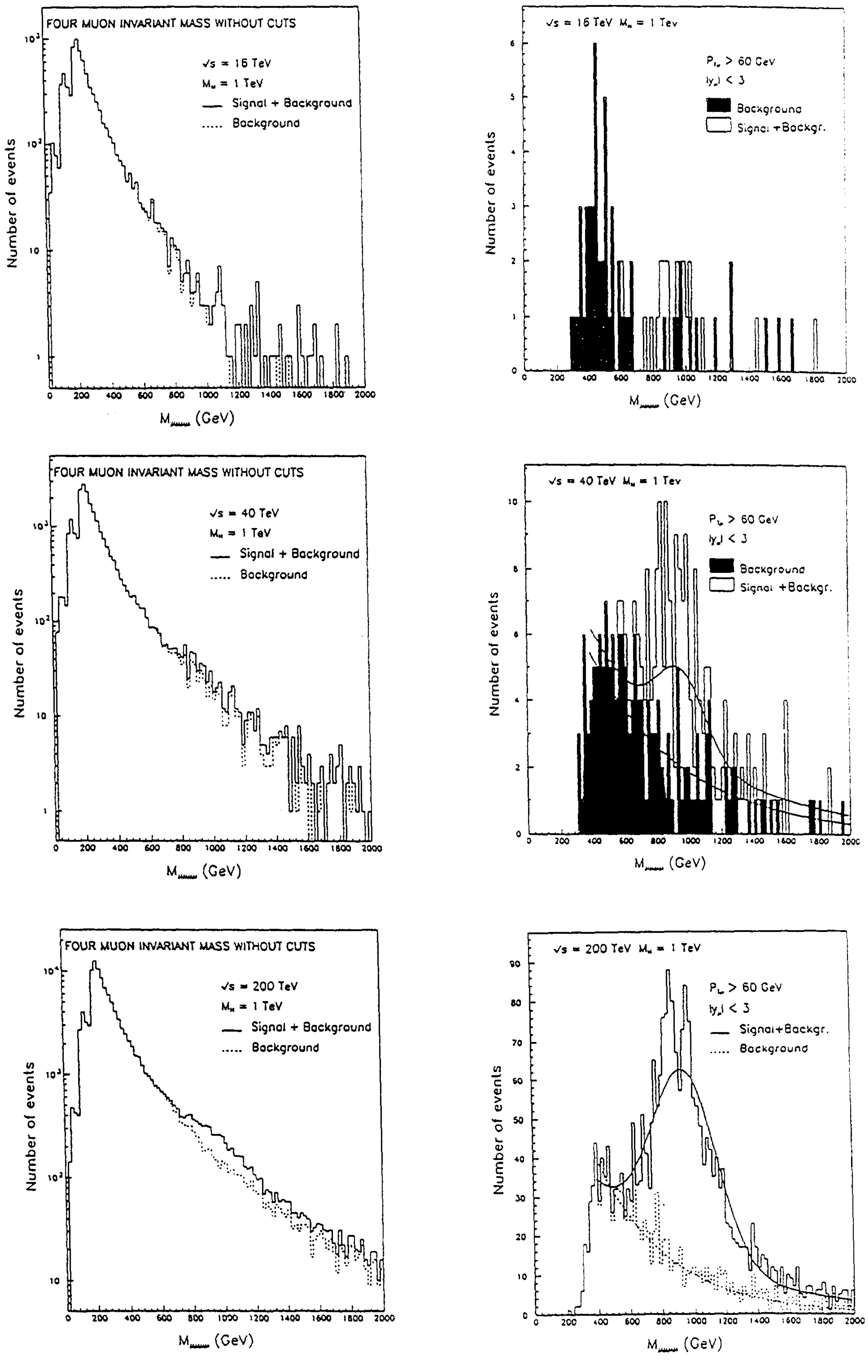
FOUR MUON INVARIANT MASS WITHOUT CUTS
√s = 16 TeV
M_H = 1 TeV
Signal + Background
Background
Number of events
M_μμμμ (GeV)
√s = 16 TeV M_H = 1 Tev
P_tμ > 60 GeV
|y_μ| < 3
Background
Signal +Backgr.
FOUR MUON INVARIANT MASS WITHOUT CUTS
√s = 40 TeV
M_H = 1 TeV
Signal + Background
Background
√s = 40 TeV M_H = 1 Tev
FOUR MUON INVARIANT MASS WITHOUT CUTS
√s = 200 TeV
M_H = 1 TeV
Signal + Background
Background
√s = 200 TeV M_H = 1 TeV
Signal+Backgr.
Background

Figure 12

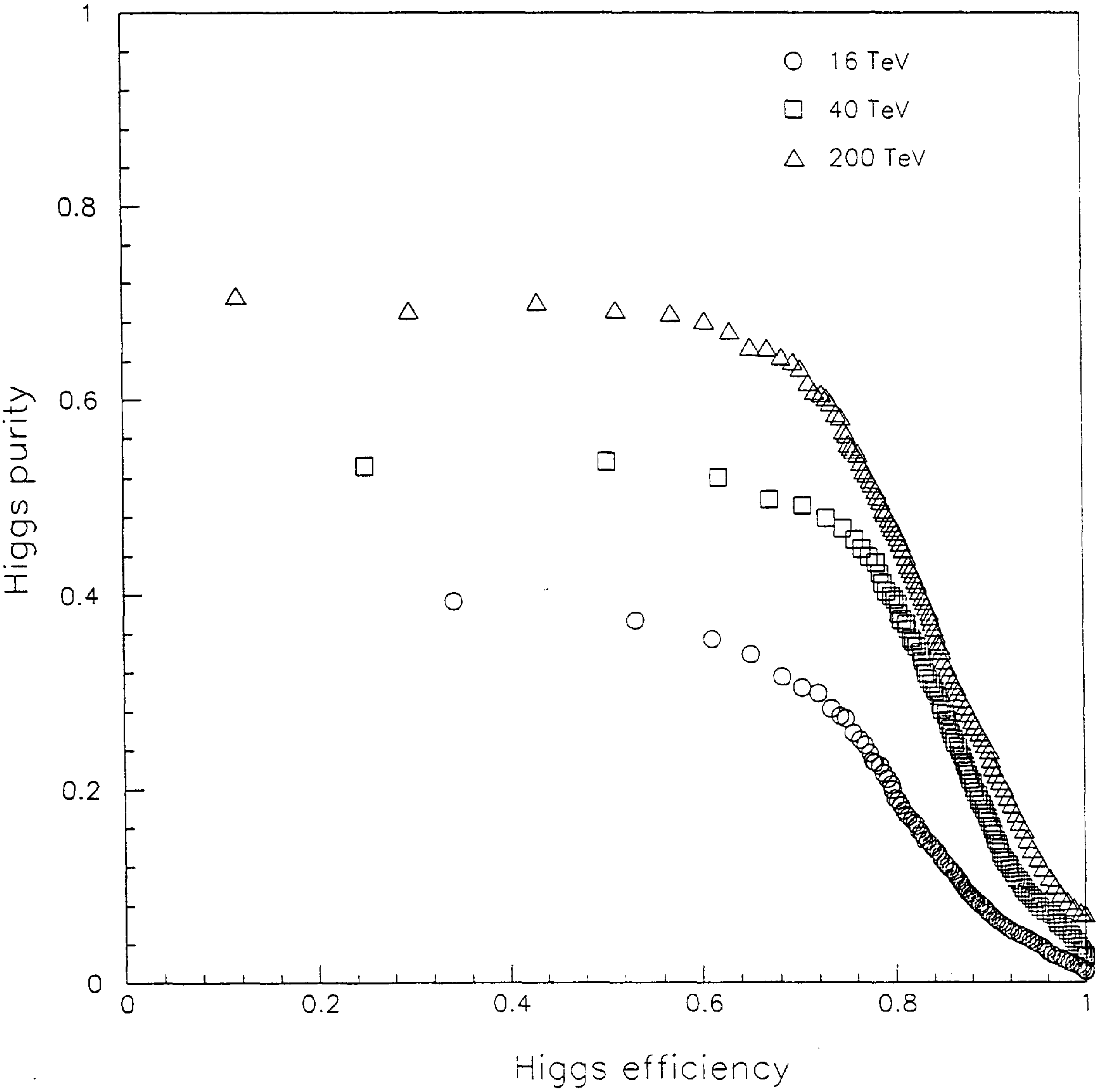

16 TeV
40 TeV
200 TeV
Higgs purity
Higgs efficiency
0
0.2
0.4
0.6
0.8
1

Figure 13

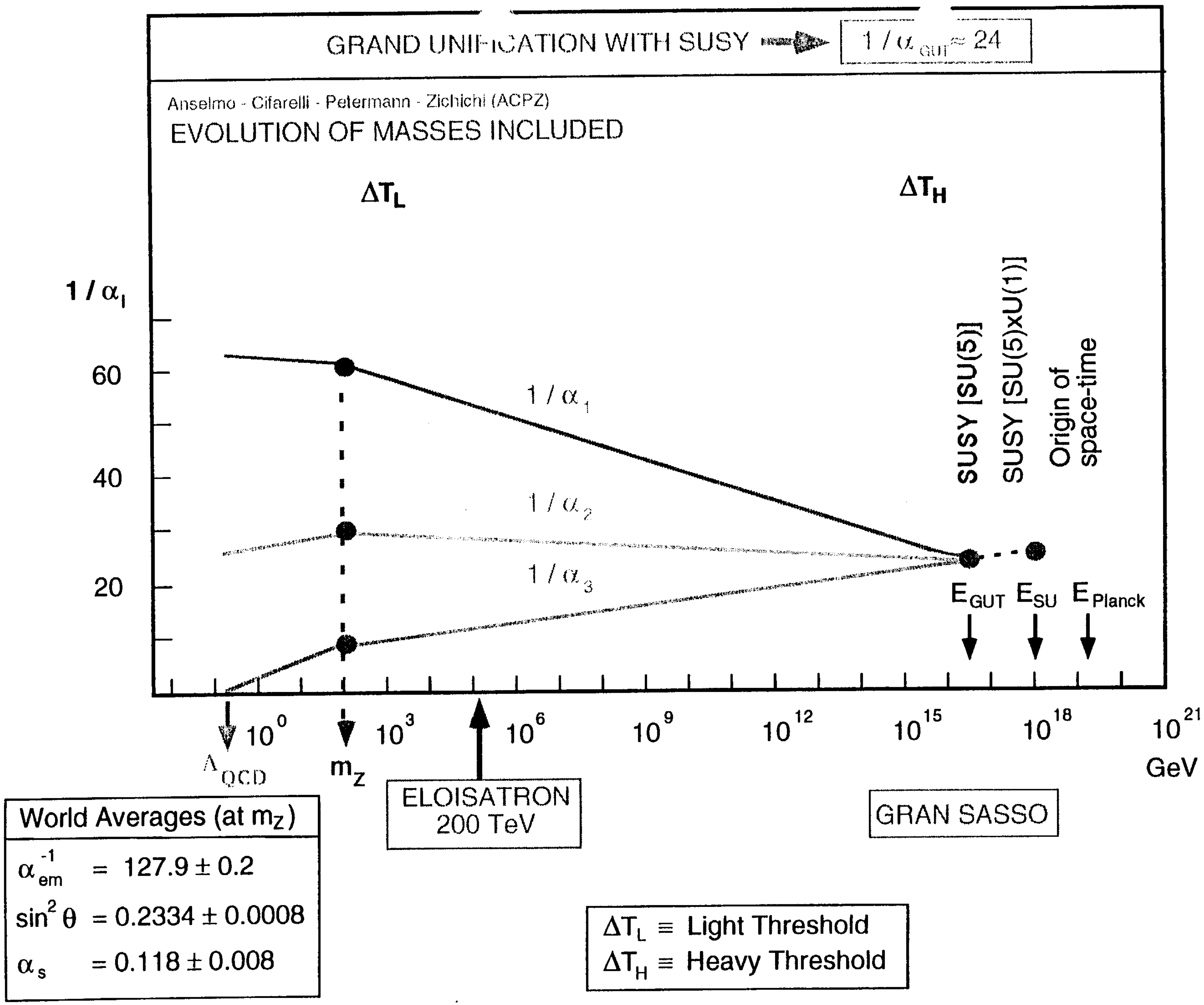

GRAND UNIFICATION WITH SUSY
1 / α GUT ≈ 24
Anselmo - Cifarelli - Petermann - Zichichi (ACPZ)
EVOLUTION OF MASSES INCLUDED
ΔT_L
ΔT_H
1 / α_i
60
40
20
1 / α_1
1 / α_2
1 / α_3
SUSY [SU(5)]
SUSY [SU(5)xU(1)]
Origin of space-time
E_GUT
E_SU
E_Planck
10^0
10^3
10^6
10^9
10^12
10^15
10^18
10^21
GeV
Λ_QCD
m_Z
ELOISATRON 200 TeV
GRAN SASSO
World Averages (at m_Z)
α_em^-1 = 127.9 ± 0.2
sin^2 θ = 0.2334 ± 0.0008
α_s = 0.118 ± 0.008
ΔT_L ≡ Light Threshold
ΔT_H ≡ Heavy Threshold

Figure 14

SUSY PARTICLE MASS SPECTRUM

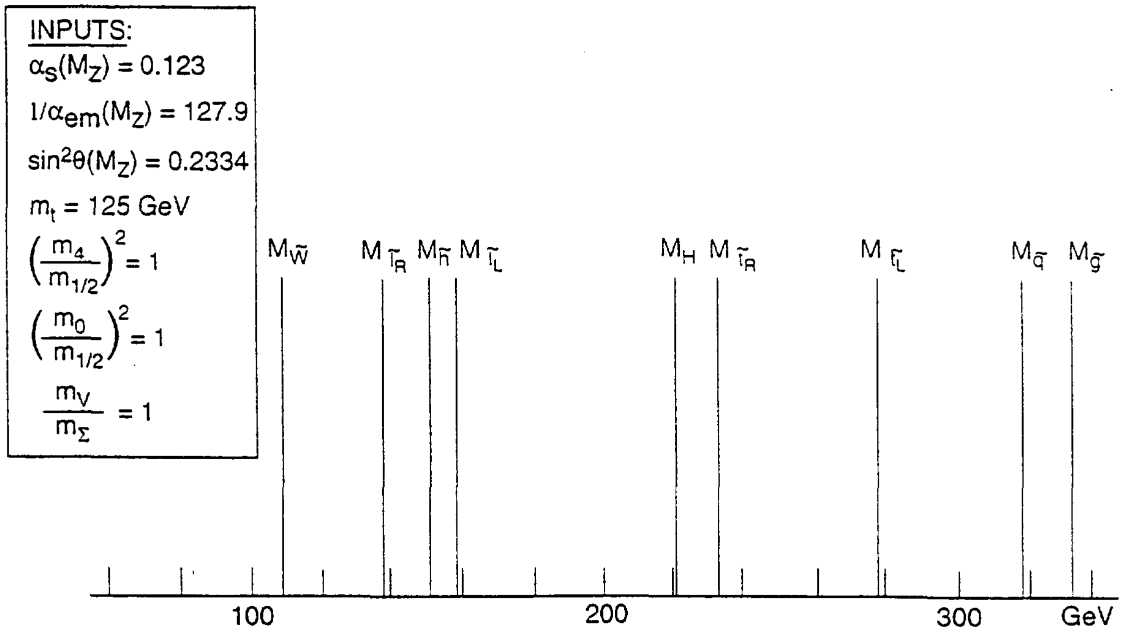

SUSY PARTICLE MASS SPECTRUM

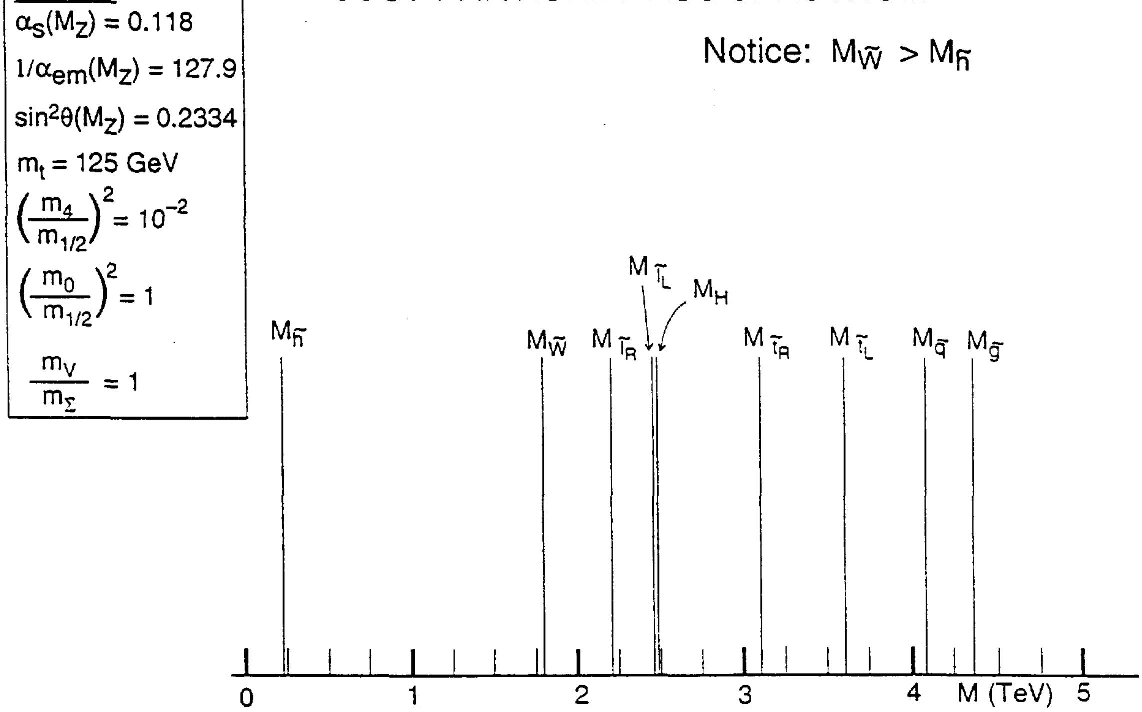

Figure 15

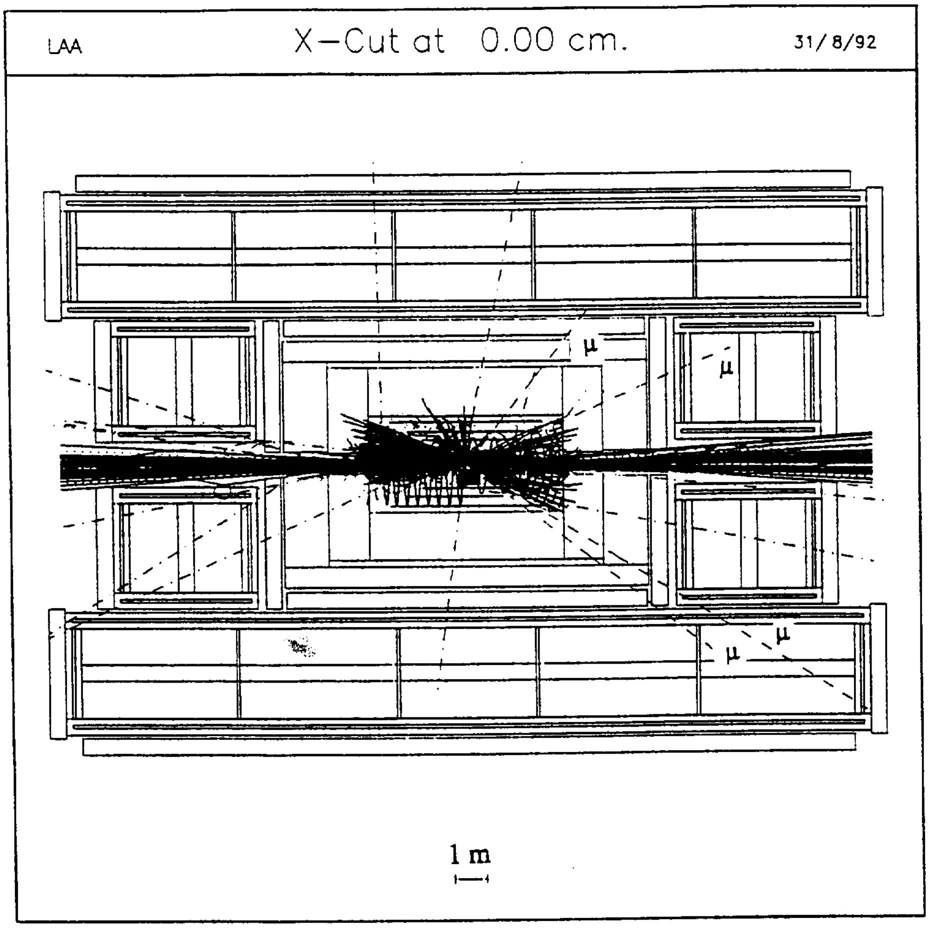
LAA
X–Cut at 0.00 cm.
31/8/92
μ
μ
μ
μ
1 m

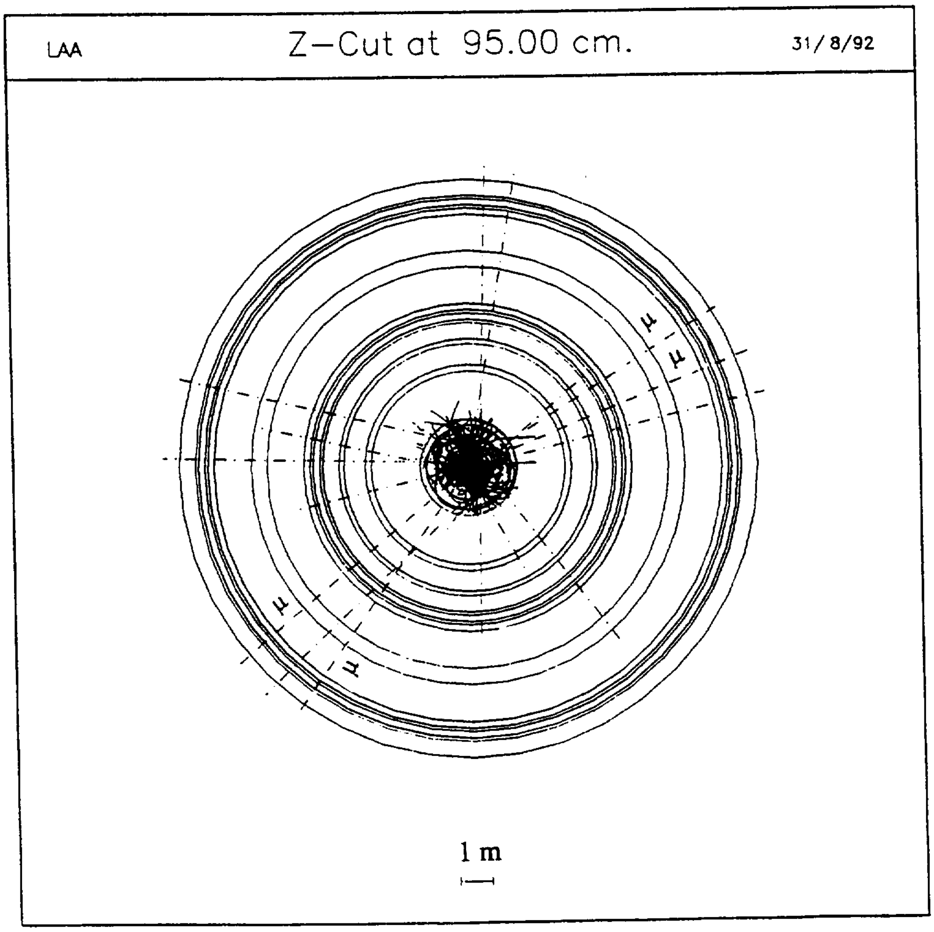
LAA
Z–Cut at 95.00 cm.
31/8/92
μ
μ
μ
μ
1 m

Figure 16

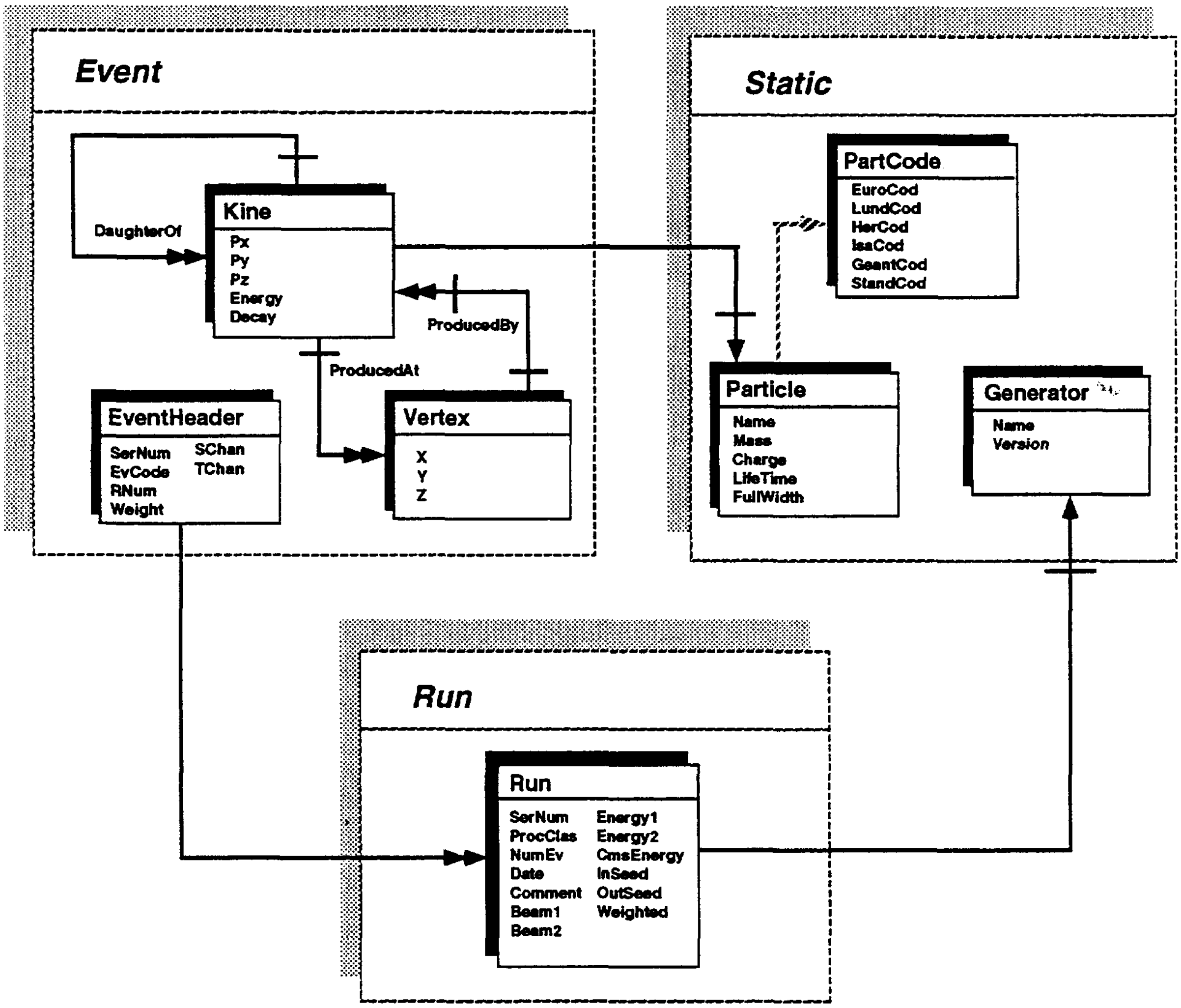
Event
Kine
Px
Py
Pz
Energy
Decay
DaughterOf
ProducedBy
ProducedAt
EventHeader
SerNum
EvCode
RNum
Weight
SChan
TChan
Vertex
X
Y
Z
Static
PartCode
EuroCod
LundCod
HerCod
IsaCod
GeantCod
StandCod
Particle
Name
Mass
Charge
LifeTime
FullWidth
Generator
Name
Version
Run
Run
SerNum
ProcClas
NumEv
Date
Comment
Beam1
Beam2
Energy1
Energy2
CmsEnergy
InSeed
OutSeed
Weighted

Figure 17

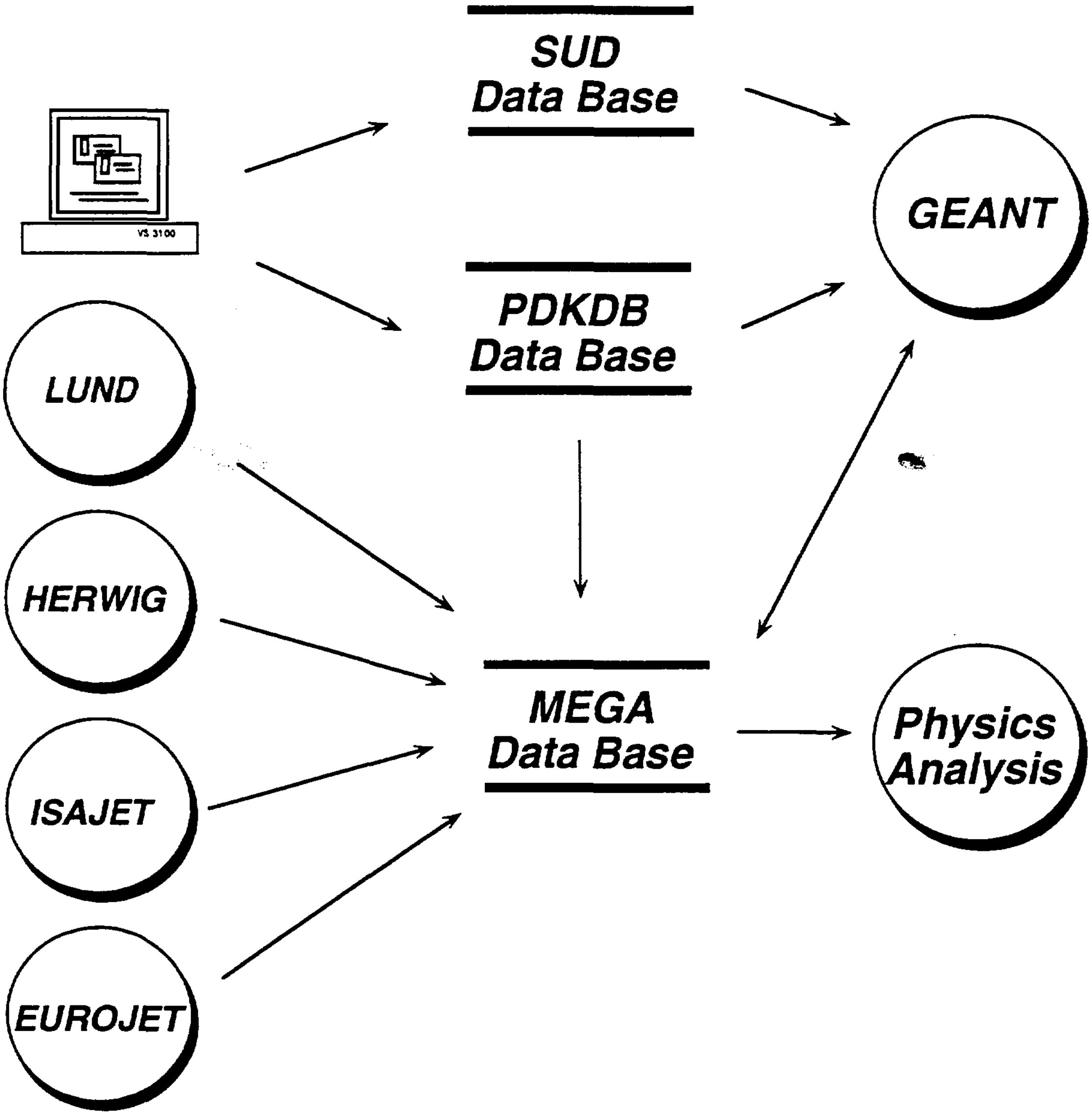

MEGA = Monte carlo Event Generator Adaptor
SUD = Set-Up Descriptor
PDKDB = Particles & Decays Data Base

Figure 18